Internal Report
DESY-CELLO-83-01
PRC 83/01
March 1983

Eigentum der Property of DESY Bibliothek library
Zugang: Accessions: - 7. JUNI 1983
Leihfrist: Loan period: 7 Tage days

PROPOSAL

TO UPGRADE THE CELLO DETECTOR

CELLO Collaboration
Behrend, H.J.

DESY behält sich alle Rechte für den Fall der Schutzrechtserteilung und für die wirtschaftliche Verwertung der in diesem Bericht enthaltenen Informationen vor.

DESY reserves all rights for commercial use of information included in this report, especially in case of filing application for or grant of patents.

"Die Verantwortung für den Inhalt dieses
Internen Berichtes liegt ausschließlich beim Verfasser"

Proposal
to upgrade the CELLO detector

CELLO Collaboration

Hamburg, March 9th, 1983

Abstract

Major modifications to the CELLO detector are proposed to meet the demands for future physics at PETRA up to beam energies of 22 GeV or even 30 GeV. The upgraded components concern the central tracking device and the forward region of the detector. The physics objectives with these improvements are discussed.

CELLO Collaboration

H.-J.Behrend, J.Bürger, L.Criegee, G.Franke, M.Gaspero[1],
J.Meyer, V.Schröder, H. Sindt, B.Stella[1],
U. Timm, G.G.Winter, W.Zimmermann
Deutsches Elektronen Synchrotron DESY, Hamburg, Germany

P.J.Bussey, J.B.Dainton, D.Hendry, C.Raine, J.M.Scarr,
I.O.Skillicorn, K.M.Smith
Department of Natural Philosophy, University of Glasgow, U.K.

V.Blobel, D.Burkart, M.Poppe, H.Spitzer
II.Institut für Experimentalphysik, Universität Hamburg, Germany

O.Achterberg, G.d'Agostini, W.-D.Apel, J.Engler, G.Flügge, D.C.Fries,
W.Fues, G.Hopp, M.Krüger, H.Müller, H.Randoll,
G.Schmidt, H.Schneider
Kernforschungszentrum Karlsruhe und Universität
Karlsruhe, Germany

W.de Boer, G.Buschhorn, G.Grindhammer, P.Grosse-Wiesmann,
B.Gunderson, C.Kiesling, R.Kotthaus, H.Lierl, D.Lüers,
H.Oberlack, P.Schacht
Max-Planck-Institut für Physik und Astrophysik, München, Germany

G.Bonneaud, A.Cordier, M.Davier, D.Fournier, J.F.Grivaz,
J.Haissinski, V.Journé, F.LeDiberder, U.Mallik, J.-J. Veillet
Laboratoire de l'Accélérateur Linéaire, Orsay, France

J.H.Field[2], R.George, M.Goldberg, O.Hamon, F.Kapusta,
F.Kovacs, L.Poggioli, M.Rivoal
Laboratoire de la Physique Nucléaire et Hautes Energies,
Université de Paris, France

R.Aleksan, J.Bouchez, G.Carnesecchi, G.Cozzika, Y.Ducros, A.Gaidot,
P.Jarry, Y.Lavagne, J.Pamela, J.P. Pansart, F.Pierre
Centre d'Etudes Nucléaires, Saclay, France

G.Alexander, G.Bella, Y.Gnat, J.Grunhaus
Department of Physics and Astronomy, Tel Aviv University, Israel

[1] Rome University, Italy
[2] on leave of absence from DESY, Hamburg, Germany

CONTENTS

1.0 INTRODUCTION

The CELLO detector has been designed to identify and measure simultaneously leptons, photons and hadrons over almost the entire solid angle. This aim is realized by the following main components:

- thin superconducting coil giving a high magnetic field,
- tracking device with proportional and drift chambers,
- lead-liquid argon calorimeters,
- hadron filter and muon-detectors,
- small angle forward detectors.

Although these components have operated satisfactorily during the past four years, we propose here major modifications of our detector in order to meet the requirements of a second generation experiment at PETRA, namely:

- operation at higher energies (up to 22-30 GeV per beam) and thus better momentum resolution in more complicated events,
- operation with higher and more complicated background rates,
- ability to aim for different and new physics issues compared to the time of the proposal of the first generation of PETRA experiments (1976).

We propose

1. to replace the central tracking device by a cylindrical drift chamber with high momentum and vertex resolution, and
2. to modify the forward detection system in the polar angle range $50 < \vartheta < 110$ mrad by using BGO shower counters with additional tube chambers, and by installing an existing shower counter in the range $26 < \vartheta < 50$ mrad.

The other components of the CELLO detector remain well suited to meet the requirements of the next five to six years of physics at PETRA.

With these modifications the CELLO detector will have the following improved features:

- charged particle measurement with a momentum resolution of $\sigma(p)/p^2 = 0.5\%\ GeV^{-1}$,

- track reconstruction down to polar angles of 140 mrad,
- multihadron event reconstruction with a track finding probability of > 95%,
- almost complete calorimetric measurement of electro-magnetic showers at all polar angles > 26 mrad.

The modifications in the forward region are intended to allow for more detailed studies of 2γ-physics and to meet better the requirements of this relatively new and growing field in e^+e^- physics as discussed during the recent meetings of the PRC.

Furthermore the proposed new components allow a flexible response to future physics issues or to different background conditions.

The modifications are such that the CELLO detector can run continuously. The new components will be installed at shutdown times. They will be fully operational in summer 1985; thus we will have at least two years of operation before the LEP experiments start data taking. Beyond that time it can be envisaged that the CELLO detector may play a role as a first generation detector at the HERA collider.

The CELLO Collaboration has been enlarged in autumn 1982 by five new groups, namely the Universities of Glasgow, Hamburg and Tel Aviv and the DESY groups F14 and F33, which were all members of the former PLUTO-Collaboration.

2.0 PHYSICS OBJECTIVES

In this section we discuss some physics issues which will be of importance during the coming years of running at PETRA. There are two main items: e^+e^--annihilation and 2γ-interactions. Both of which are fields of considerable importance in high energy physics today. In the context of this proposal we merely mention briefly the relevant ideas without going into details. We infer from these physics topics the required detector properties. These properties are compiled and translated into technical specifications in the next section.

2.1 ELECTRON-POSITRON-ANNIHILATION

We discuss below the following physics questions:

- Is QCD a valid description of strong interactions?
- How do partons fragment into the observed particles?
- How big are the effects from electroweak interactions?

Two further items which would be very important if positive results were found should be added to the above mentioned questions:

- the search for exotic particles, in particular new heavy leptons and the Higgs boson,
- the search for the sixth quark t.

2.1.1 QCD Studies

One aspect of this subject is the more detailed study of the nature of multijet events. Another is the extraction of relevant information from correlations of the particles in an event. The aim is to determine the strength and the energy dependence of the strong coupling constant.

Apart from the question of how well one can identify jets found in an event with the underlying parton configuration, event shapes and single particle distributions have to be studied. The quality of such an analysis is worsened by bad momentum resolution and inefficient track reconstruction. It turns out that badly measured or wrongly reconstructed tracks make the analysis of e.g. charge-correlations complicated. For this type of physics a

good momentum resolution for almost all particles within a high multiplicity hadronic event is required.

2.1.2 Fragmentation of Partons

The study of parton fragmentation which is intimately connected to the study of QCD will remain a central issue in hadronic e^+e^--annihilation. The main task will be to disentangle carefully single jets and study them from two points of view:

- to explore the differences between quark- and gluon jets
- to measure as many jet properties as possible to find a good description of the fragmentation process.

Refined measurements of the final state are needed in order to discriminate between different models of the fragmentation process /1/. Good momentum resolution and event reconstruction will play a dominant role. Of course, particle identification would be also desirable. Within the given limitations of the detector, only low momentum particles can be identified by time of flight counters or ionisation measurement. The main objective of CELLO will therefore be the reconstruction of primary mesons and baryons like ρ, D, D^*, K^0_s etc., where again momentum resolution will be of supreme importance, and the limited particle identification will only be a supplementary aid.

2.1.3 Electroweak Effects

At PETRA the theory of electroweak interactions can be tested by observing interference effects between electromagnetic and weak neutral current processes. Since the measurable effects grow with s, such tests become more and more important as the PETRA energy increases. Electroweak effects can be studied in both lepton- and quark pair production.

2.1.3.1 Production of Lepton Pairs

Three kinds of reaction are experimentally accessible:

1. $e^+e^- \rightarrow e^+ e^-$
2. $e^+e^- \rightarrow \mu^+\mu^-$
3. $e^+e^- \rightarrow \tau^+\tau^-$

Measurements of the total cross sections of these processes probe the weak vector coupling constants v_i of the leptons (i = e, μ, τ). In the standard model of electroweak interactions the v_i are expected to be very small, resulting in a limited sensitivity of the total cross section measurement to electroweak effects. The axial vector coupling constants a_i of μ and τ, however, can be determined by measuring the angular asymmetry A_{fb} of the lepton pairs produced in reactions 2 and 3. Present experimental results ($a_\mu^2 = 1.24 \pm 0.16$) are in good agreement with the standard model ($a_\mu^2 = 1.00$) /2/.

In view of the increasing PETRA energies, μ-pair production is of special interest since the achievable experimental accuracy on $A_{\mu\mu}$ may provide a measurement of the Z_0 mass (due to the sensitivity to the propagator effect). Present data are compatible with $m(Z_0) = \infty$. within 2.6 standard deviations.

To determine the sign of the final state high energy muon unambiguously, high momentum resolution in the central track detector is essential. Compared to the present CELLO detector a time-of-flight system could significantly reduce the cosmic ray muon background.

CELLO has been able to measure the asymmetry $A_{\tau\tau}$ in τ-pair production with an accuracy comparable to that of $A_{\mu\mu}$, due to its good angular coverage for both charged and neutral particles and its very low trigger bias. A precise measurement of this reaction is very important since it checks lepton universality ($a_\tau = a_\mu$) and also provides the possibility to determine the final state lepton polarization. A measurement of a parity violating quantity like the polarization provides information on the product of vector and axial vector coupling constants and thus gives a valuable additional constraint on both quantities. First measurements on τ-polarisation are already available from CELLO. /3/. Again, to improve these measurements, good momentum resolution is necessary.

2.1.3.2 Electroweak Effects in Quark Pair Production

The primary goal is to measure the coupling of the Z_0 to heavy quarks. As in the case of lepton pair production a measurement of the total cross section provides only limited sensitivity to weak quark couplings. The expected effects are small and have to be disentangled from QCD corrections. A more promising way is a measurement of quark asymmetries. According to the standard electroweak theory the expected asymmetry in fermion pair production due to electroweak interference is inversely proportional to the charge of the produced fermion. This means that the expected asymmetries for heavy quark pair production are quite sizeable

(at $\sqrt{s}$ = 35 GeV: A_{cc} = -14%, A_{bb} = -27%). The crucial experimental point is how to tag the charges and flavour of the produced quark. Two experimental approaches have been adopted:

(i) Identify the flavour of produced hadrons:

This has been shown to be possible for charmed mesons by measuring in the decay sequence:

$$D^{*+} \rightarrow D^0 \pi^+ \rightarrow K^- \pi^+ \pi^+$$

the mass difference between the $K^-\pi^+$ and $K^-\pi^+\pi^+$ state /4/. A high resolution track detector can identify this process more efficiently because of its improved rejection of combinatorical background.

(ii) Identify the quark flavour in semileptonic decays:

Inclusive lepton searches provide the possibility to determine the flavour of the parent quark. Cuts on the transverse momentum of the lepton with respect to the jet axis of the event allow a discrimination to a certain extent between charm, bottom and heavier quarks. The detector has to measure precisely the jet direction and the lepton momentum. Lepton (e, μ) identification could use the muon chambers and the dE/dx capabilities of the central track detector and the liquid argon calorimeter.

2.1.4 Search for Exotic Particles

In gauge theories of particle physics the existence of scalar particles, e.g. Higgs bosons, has a key function in the understanding of particle masses. Several searches for new particles have been performed at PETRA so far. None of them have found positive evidence for any new particle and many proposed particles have been excluded within the present PETRA energy range. But there remains a considerable number of possibilities (e.g. the existence of photinos, and some kinds of neutral leptons) which have not been ruled out so far experimentally. Future searches therefore require better statistics and better detectors. For many processes, (e.g. searches for new leptons), an almost complete angular coverage with electromagnetic calorimeters is required to suppress QED background.

In the proposed layout CELLO will have an almost complete coverage down to 26 mrad. Triggering on single low energy electrons and photons, e.g. as required by searches for supersymmetric particles, is provided by the lead-liquid argon calorimeters. Together with its excellent e- and

μ-detection capabilities CELLO will be an ideal detector for refined searches for new particles.

2.1.5 Top-Physics

In 1985 it will certainly be known whether the top quark mass lies within the beam energy range available at PETRA. Even if it has been already discovered, a lot of exciting physics will remain to be done, frequently requiring outstanding detector performance.

2.1.5.1 Toponium studies

Toponium (ψ_t) will provide a unique laboratory to study the validity of QCD and gluon jets through the decay into three gluons (ggg) and the radiative decay into a photon and two gluons (γgg). The detector requirements for these studies have been discussed in the sections "Fragmentation of Partons" on page 4, and "Search for Exotic Particles" on page 6.

The radiative decay of the excited state of toponium (ψ'_t) will be extremely difficult to observe inclusively. However, it will be possible to see the double cascade

$$\psi'_t \rightarrow \gamma\chi_t \rightarrow \gamma\gamma\psi_t \rightarrow \gamma\gamma + l^+l^-$$

where $l^\pm$ is a lepton, thanks to the excellent granularity of the liquid argon calorimeter, its 4π coverage, and its capability to detect low energy photons. However, it will be necessary to keep the amount of material inside the coil as small as possible, and also to obtain a very good angular resolution for the charged leptons.

It will be extremely interesting to look for exotic decays such as $\psi_t \rightarrow \gamma H^\circ$, where H° is a Higgs boson. The energy resolution of the electromagnetic calorimeter is of paramount importance to demonstrate the existence of such a decay. Good pattern recognition capability and track momentum resolution will also be very valuable to study the subsequent decay of the H°, most likely to $\tau^+\tau^-$ or b $\bar{b}$ pairs.

The study of the reaction

$$\psi'_t \rightarrow \pi^+\pi^-\psi_t \rightarrow \pi^+\pi^-\nu\bar{\nu}$$

gives the possibility of counting the number of neutrinos. A highly efficient trigger on low $p_\perp$ tracks and a large acceptance for charged and neu-

tral particles will be needed for this measurement. A by-product could be a very substantial improvement of the present lower limit on the gravitino mass, since the rate of the decay $\psi_t \rightarrow$ gravitino + antiphotino goes like $M^4(\psi_t)/m^2(\text{gravitino})$.

2.1.5.2 Open top studies

Production of top mesons will yield high multiplicity events, the complete reconstruction of which will need a good pattern recognition power. The identification and study of excited top mesons will also require a good ability to detect and measure very low momentum pions.

The study of the semi leptonic weak decays of the top quark, in order to measure the Kobayashi-Maskawa angles and phases, will be of particular interest. Good e/π separation for high energy electrons will be extremely important. For this not only the good granularity and energy resolution of the electromagnetic calorimeter will be required, but also correspondingly good momentum resolution for charged tracks.

2.2 2γ-INTERACTIONS

In recent years 2γ-interactions have turned out to be a very interesting area of physics which is quite complementary to 1γ-annihilation. The importance of this field has been pointed out several times by the PRC. As far as the CELLO collaboration is concerned, a considerable fraction of our work has gone into this field. In particular we have results on:

- f_0, A_2, η' - resonance production /5/
- $\rho_0\rho_0$ production near threshold /5/
- the photon structure function F_2 /6/

Our future plans concerning 2γ-physics with CELLO were communicated to the PRC in the document PRC 82/10 of July 9, 1982 "Future Prospects of Two Photon Physics with the CELLO Detector". Since then the CELLO collaboration has been enlarged by groups with experience and interest in this field.

We shall now briefly review the physics of 2γ-interactions with emphasis on open questions. We discuss the following topics: resonance production and exclusive states, total 2γ-cross sections, the photon structure function and high transverse momentum jets.

2.2.1 Resonance Production and Exclusive States

The states that can be produced in 2γ-interations have an even charge conjugation parity and spin not equal to 1. The resonances η', f^0, A_2 and f' have been studied by various groups /5,7/. In all cases the 2γ-widths, $\Gamma_{\gamma\gamma}$, have large errors due to small statistics and systematic errors including the lack of understanding of the background under the resonance. In general, the $\Gamma_{\gamma\gamma}$-values reflect the quark composition and structure of the mesons, and a variety of theoretical predictions exist.

In the future it will be of interest to search for hidden charm states such as the η_c and the ψ's, and also to look for the direct 2γ-production of glueball candidates such as then $\iota(1440)$ observed in the $K^+K^-\pi^0$ channel by the Crystal Ball Collaboration /8/. Glueball states are expected to have lower values of $\Gamma_{\gamma\gamma}$ than the $q\bar{q}$ states, so that even the measurement of an upper limit on $\Gamma_{\gamma\gamma}$ can provide valuable confirmatory evidence of their gluonic nature. The best experimental signature for the $\iota(1440)$, e.g. would be the decay channel $K^0_s K^\pm\pi^\mp$. To extract a clean $K^0_s \rightarrow \pi^+\pi^-$ signal, as well as to find the narrow mass peaks expected from hidden charm production in exclusive final states such as 4π and $K\bar{K}\pi\pi$, a good momentum resolution is crucial to reject combinatorical backgrounds.

Particle identification capability particularly for momenta below 1 GeV is very important for low multiplicity 2γ-physics. Examples are the efficient rejetion of beam gas background by removing events with slow protons, and the identification of exclusive 2 body final states such as $p\bar{p}$ /9/ and K^+K^- /10/.

As far as multiparticle exclusive channels are concerned the channel $\gamma\gamma \rightarrow \pi^+\pi^+\pi^-\pi^-$ has generated the greatest interest due to the observation of both an unexpectedly large cross section for the production of $\rho^0\rho^0$ states near threshold and the evidence for a narrow structure at 2.1 GeV /11/. It has recently been suggested that the large $\rho\rho$ cross section may be due to VDM effects /12/. In this case a hitherto unobserved and large cross section for $\gamma\gamma \rightarrow \omega\omega$ near threshold should also exist. For detailed studies of the reactions, the detector is required to have a good acceptance near the forward direction. In addition since we are dealing with low momentum, the trigger must accept particles with low transverse momenta.

2.2.2 Total 2γ-Cross Section

Preliminary total 2γ-cross sections have been presented by two groups /13/. There is substantial disagreement. The problem is in the determi-

nation of the acceptance of low multiplicity events in particular and in finding a model to adequately describe the final hadronic system. A point of considerable importance in the total cross section measurement is the determination of its Q^2 dependance. It is of interest to measure carefully the transition from the rapid Q^2 dependence of the VDM region to the slower one of the pointlike 2γ-interaction. At both low and high Q^2 it will also be of interest to see if the $1/W^2$ dependence expected from pointlike interactions is observed.

2.2.3 Photon Structure Function F_2

The interest in the structure function lies in the expectation that it can be calculated to a good approximation in perturbative QCD, both in shape and magnitude, given the value of Λ. Measurements so far are in substantial agreement with QCD predictions /6,14/ but yet are unable to establish the expected logarithmic Q^2 dependence /15/. A good measurement of the structure function at large x, where the differences between the quark-parton model and QCD are largest, requires an understanding of the acceptance at low W and high Q^2. Determination of the Q^2 dependence requires measurements of the tagged electron over a large angular range, thus requiring a small angle tagging device. The CELLO liquid argon endcap calorimeters will act as good tagging devices at high values of Q^2.

We have studied the expected resolution in W and x with Monte Carlo methods. Figure 1 and Figure 2 on page 12 show the distributions of W_{vis}/W for the 1983 version of CELLO and for the proposed one. W_{vis} is the energy of the 2γ-system as reconstructed from the detected charged and neutral particles in the central detector and in the shower counters. Figure 3 and Figure 4 on page 13 show the corresponding distributions of x/x_{vis}. In particular at low W and high x a good resolution will be obtained.

With the good acceptance for the final state particles to be expected in the upgraded CELLO detector, and a sufficiently high integrated luminosity, detailed studies of the final state in high Q^2 single tag events will become possible. Evidence can be sought for the expected 2-jet structure (one jet at high $p_\perp$, the other in the beam direction). The flavour tasting techniques mentioned above in Sec. " Electroweak Effects in Quark Pair Production" on page 5 can be used to measure directly the contribution of charmed quarks to F_2. A good momentum resolution, as well as an efficient electron recognition for all energies are clearly of great importance for such studies.

2.2.4 High Transverse Momentum Jets

The observation of jets with $d\sigma/dp_\perp^2 \sim p_\perp^{-4}$ is predicted by QCD. Such jets can be due either to a highly virtual photon or to the exchange of an off-mass-shell quark. The first case corresponds to the photon structure function as described above. In both these cases the VDM part of the 2γ-interactions should make negligible contribution. Several PETRA experiments have reported on the jets resulting from the exchange of off-mass-shell quarks, but with low statistics /16/. To date neither detailed jet topology, nor their Q^2 dependence has been studied. In all experiments an excess of high $p_\perp$ jets over the lowest order prediction is observed. It remains to be seen whether this excess can be understood in terms of a VDM 2γ-interaction alone.

The tagging of high-$p_\perp$ jets becomes difficult for energies $W \geq 10$ GeV. Here the tagging rates for energies of the scattered electrons of > 6 GeV are comparable to the rate of high energy photons radiated from 1γ-annihilation events. We therefore aim at identifying photon initiated showers (e/γ separation) in the range $30 < \vartheta < 105$ mrad. This measure also improves the acceptance of final state (soft) photons from 2γ-processes.

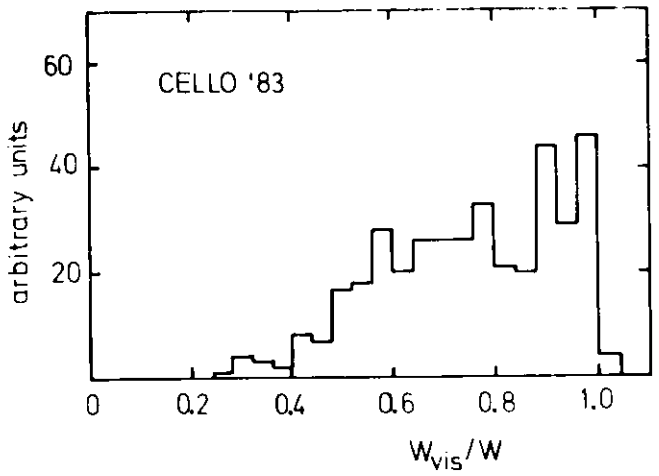

Figure 1. Distribution of W_{vis}/W for the 1983 version of CELLO: from deep inelastic $e\gamma$ scattering events (E_{beam} = 17 GeV; $E_{e'}$ > 7 GeV; u-, d-, s-, c-quarks with LUND-fragmentation).

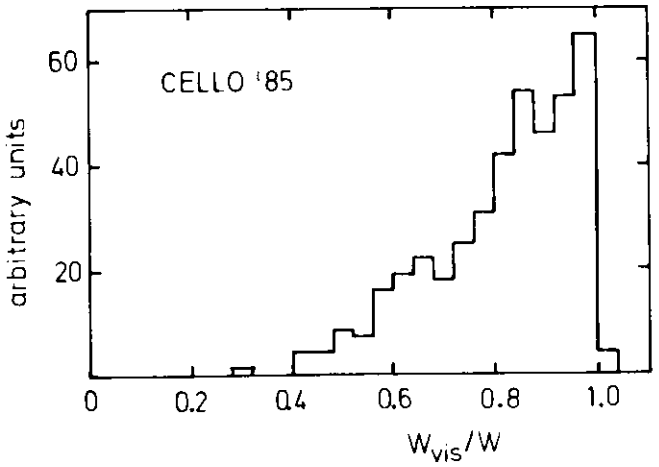

Figure 2. Distribution of W_{vis}/W for the proposed version of CELLO: from deep inelastic $e\gamma$ scattering events (E_{beam} = 17 GeV; $E_{e'}$ > 7 GeV; u-, d-, s-, c-quarks with LUND-fragmentation).

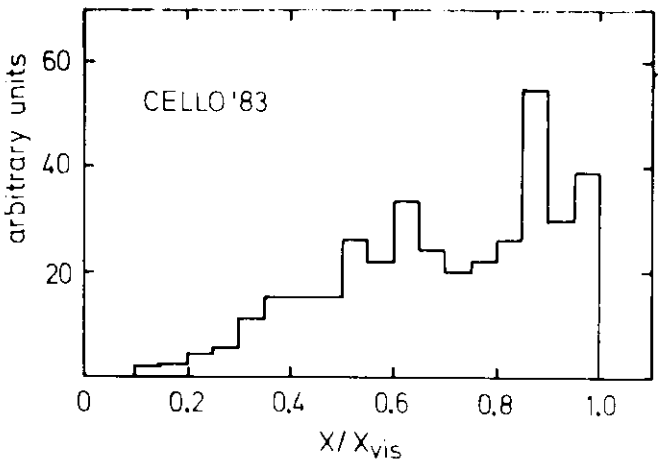

Figure 3. Distribution of x/x_{vis} for the 1983 version of CELLO: from deep inelastic $e\gamma$ scattering events (E_{beam} = 17 GeV; $E_{e'}$ > 7 GeV; u-, d-, s-, c-quarks with LUND-fragmentation)

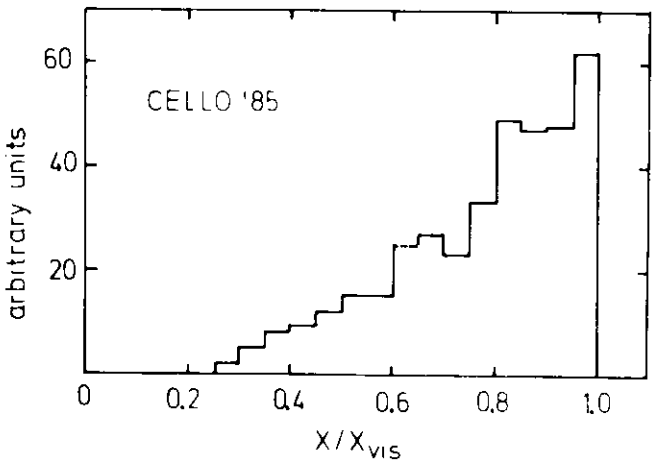

Figure 4 Distribution of x/x_{vis} for the proposed version of CELLO: from deep inelastic $e\gamma$ scattering events (E_{beam} = 17 GeV; $E_{e'}$ > 7 GeV; u-, d-, s-, c-quarks with LUND-fragmentation).

3.0 SPECIFICATION OF THE NEW DETECTOR COMPONENTS

From the physics aims presented above we infer the following general properties of the new detector components. They have been obtained from detailed studies of the feasibility of different solutions for the detector components with boundary conditions given by the existing hardware of the CELLO detector.

3.1 CENTRAL TRACK DETECTOR

Our choice is to build conventional cylindrical drift chambers in a single gas volume. The following general design criteria have been considered:

1. Drift Chambers

   - High momentum resolution,
   - good resolution of the reconstructed vertex,
   - good spatial resolution in case of high track densities as expected in jets with energies above 20 GeV,
   - drift cells which allow operation at high magnetic field,
   - option for dE/dx measurement,
   - easy integration into the existing CELLO trigger-system.

2. Mechanics

   - Rigid endplates, with precision drilled wire feedthroughs. These are parts of a pressure vessel which allows stable operation up to 3 bar. Hence we can operate the chambers at normal pressure independent of atmospheric changes and have the option of improving the resolution by operating at higher pressures,
   - a separate, but also internally rigid inner part, the vertex chamber, to allow a later adjustment to different beam and background conditions without changing the complete detector (The proposed setup will also minimize the material in front of the forward detectors),
   - thin beampipe as integral part of the vertex chamber,

   - space for TOF counters between pressure vessel and coil.

3. Electronics

   - Design based on existing and proven solutions (TDC, ADC), but flexible enough to allow for future extensions,
   - capability of equipping all channels with TDC, ADC and charge division readout.

4. Data Acquisition and Processing

   - Full use of existing knowledge and software solutions concerning checkout of the drift chambers, data readout and system calibration,
   - pattern recognition and track fitting on the basis of procedures which are already existing and have been well tested.

3.2 FORWARD TAGGING COUNTERS

The present tagging counter of CELLO covers the angular range from 50 to 100 mrad. It is positioned outside the endcap cryostat behind a massive flange of two radiation lengths thickness on average. Thus the Q^2 resolution of electrons is limited to 15% at $E_{e'} = 6$ GeV. It is difficult to identify showers from low energy photons.

The proposed modifications to the forward taggers are guided by the following design goals:

- extended coverage for electrons down to 26 mrad in order to provide tagging at moderate Q^2,
- a Q^2 resolution which matches that of the endcap liquid argon counters ($\sigma(Q^2)/Q^2 \sim 6\%$) (At smaller angles this requires not only a good energy resolution, but also a fine segmentation in the angle.),
- coverage of photon measurement for $E_\gamma \gtrsim 150$ MeV in the range $26 < \vartheta < 105$ mrad. This implies the ability to identify photon initiated showers (i.e. e/γ separation), and also a minimum amount of material in front of the detectors,
- radiation resistant shower counter materials.

The above mentioned massive flange of the endcap cryostat at |z| = 2200 mm cuts into the forward acceptance down to 55 mrad. Hence we choose a two step solution (as has been sketched in our note PRC 82/10):

1. A large angle forward detector (LAF) inside the endcap cryostat at |z| ~ 1500 mm covering the angular range $50 < \vartheta < 110$ mrad. This counter is exposed to a field of 0.5 to 1 T.

2. A small angle forward detector (SAF) at |z| ~ 3500 mm outside the endcap cryostat covering the angular range $26 < \vartheta < 50$ mrad.

We propose a BGO counter for region 1. In region 2 we plan to use either a modified version of the present lead glass tagging system or the small angle tagger of PLUTO which is a lead scintillator counter. The lead glass system would be shielded by ~ 1.5 cm of lead wrapped around the beampipe. If radiation damage to the lead glass cannot be prevented even by this shielding, we propose to use the PLUTO counter instead. The shower counters in region 1 and region 2 will be supplemented by 4 planes of drift and proportional chambers for e/γ separation.

3.3 BEAMPIPE

The central part of the beampipe, covering the angular range of $|\vartheta| > 130$ mrad has to be as thin as possible: a value of 0.5% to 0.8% radiation length is envisaged. This very thin part has essentially two functions:

- to allow a high precision vertex reconstruction with the central detector
- to minimize electron background from γ conversions

The twofold structure of the forward tagging counters is reflected by two windows.

The window for particles in the LAF angular range ($50 < \vartheta < 110$ mrad) will be conical. The beampipe trumpet for this window is relatively thick. It serves at the same time as a rigid wall of the vertex chamber and in combination with other absorbers installed in the beampipe as a synchrotron radiation shield for the inner detector. For the particles traversing the beampipe in the extreme forward direction ($26 < \vartheta < 50$ mrad), another window has to be installed. The necessary beampipe trumpet can be positioned downstream behind the LAF.

4.0 CENTRAL TRACK DETECTOR

The proposed central track detector was designed making widely use of the experience we have collected so far in building such detectors. It was aimed to have an improved performance in momentum and vertex resolution and in pattern recognition for events with high track densities. It should be mentioned in this context that especially the latter property is a necessary requirement for measurments of the current jet in deep inelastic ep-interactions at HERA.

Furthermore the proposed modification was guided by our experience that the existing inner detector will deteriorate in its performance due to aging effects, so that the physical capacity of the whole detector may suffer considerably.

The proposed central track detector contains 36 layers of drift chambers in a common gas volume as shown in Figure 5 on page 18, and will be referred to as 'Stereo Wire Chamber' (SWC). The beam pipe serves as the inner wall of the vessel. It consists of a thin beryllium pipe in the center, to allow for a good vertex reconstruction, followed by two cones which are thick enough to protect the volume of the central detector against synchrotron radiation produced in the mini-beta quadrupoles of PETRA. In order to allow for adaptation to future beam and background conditions, and also for possible new vertex detection techniques, the inner part is mechanically separated from the much larger outer one. The smallest angle at which coordinates of charged particles can be measured is 135 mrad.

The 36 drift layers are arranged in an uncommon way, namely 18 at +2°, none at 0°, and 18 at -2° ("18:0:18"). This choice gives an extra constraint for the track reconstruction, as compared to traditional divisions like 3:9:3 (TASSO) or 5:11:5 (new PLUTO central detector). The point is that if the the stereo angles are kept equal for all layers of one stereo view, charged particles produce circular images in that view . One can therefore perform an independent track reconstruction in the stereo view and thus increases the probability for finding a particular trajectory. The proviso is however that the stereo view contains a sufficient number of layers to allow an efficient track finding. In view of the left-right ambiguities in the drift cells the 9 layers resulting from a 9:18:9 division are marginal. A modification into a 18:18:0 division, on the other hand, gives a good track reconstruction in the stereo view, without seriously harming the traditional way of the z-reconstruction. Our preference of the proposed 18:0:18 division as compared to the 18:18:0 scheme is motivated by the better z-resolution. Detailed Monte Carlo studies have shown that the full track reconstruction in such a device is manageable.

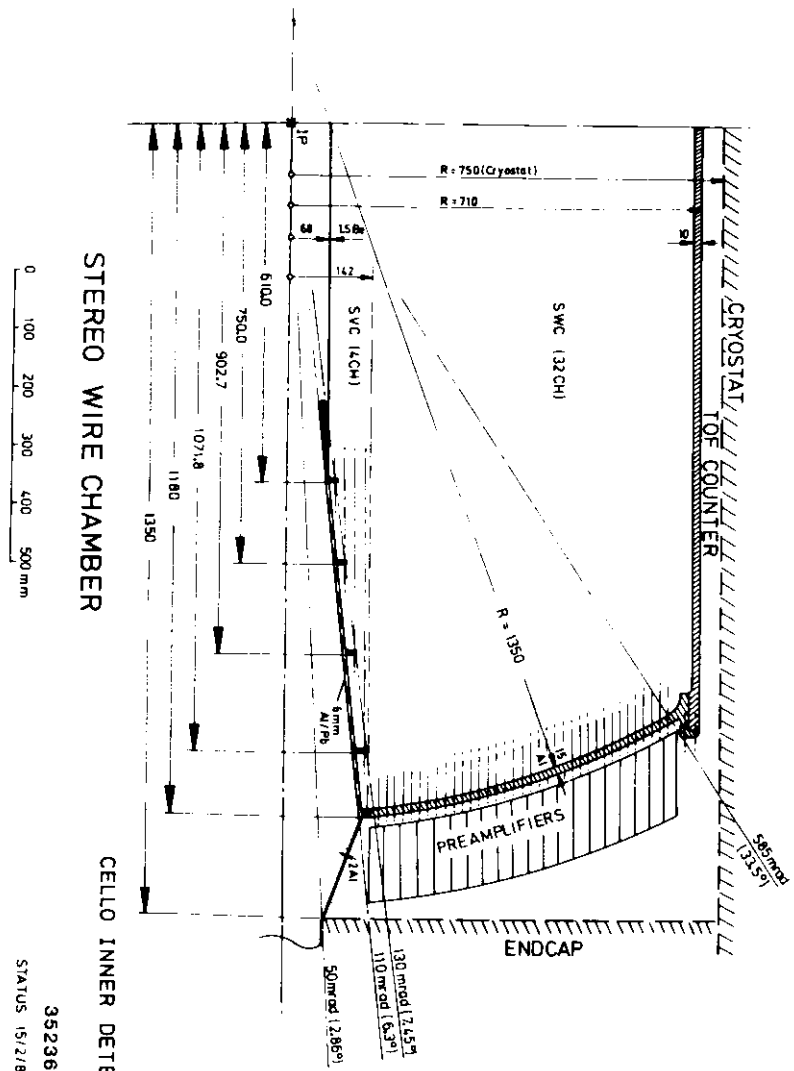

Figure 5. The Stereo Wire Chamber for CELLO

4.1 PRESSURE VESSEL

The gas vessel will be constructed for a pressure of 3 bars, an option which may be used to improve the tracking accuracy. The endflange will be thinner than that of the present CELLO central detector. Its rigidity is provided by the spherical shape. The outer diameter is chosen such as to allow the later insertion of a time of flight counter which could be useful to provide a cosmic trigger for the central detector and to reject background from cosmic rays. Details of this system are under study.

The conical part of the beam pipe obscures only the angular range from 110 to 130 mrad, which is inefficient anyway because of the cryostat of the liquid argon endcap calorimeter. The diameter of the beryllium part and of the synchrotron radiation absorbers are based on a conservative evaluation of the experience obtained in the data taking at the end of 1982. The experience of the PETRA detectors at the forthcoming higher energies may still lead to modifications. For this reason the inner part of the SWC is mechanically separated, so that the construction of the outer part which contains 96% of the wires can start without delay.

4.2 DRIFT WIRES

The arrangement of the 7488 drift cells is shown in Tbl. 1 (p.20) . The wires are arranged in hyperbolic layers, due to the stereo angle. Four layers form a block, which contains a set of two +2°- and two -2°-layers with staggered cell arrangement. Thus the inherent ambiguities of the driftcells can be resolved locally.

The shape of the cell is chosen to be hexagonal, which represents the most economical approximation of an ideal circular one. This shape has been used and extensively studied (with and without magnetic field) in the new PLUTO central drift detector. The hexagonal cell shape has very uniform drift properties in more than 60% of the cell volume, independent of the strength of the magnetic field, and thus facilitates track reconstruction. The pulse height information can in principle also be read out from the wire signals, providing dE/dx information. In our design we explicitly try to optimize the drift resolution, even at the expense of dE/dx resolution.

Nr.	Radius (z=0) (mm)	Radius (z=zm) (mm)	zm (Len/2) (mm)	Number of wires	Drift-dist. (mm)	Stereo angle (mrad)
1	78.7	81.4	596.5	80	3.09	34.9
2	94.0	97.5	736.5	80	3.69	34.9
3	110.7	115.0	889.2	80	4.35	-34.9
4	129.1	134.3	1058.3	80	5.07	-34.9
5	152.0	157.3	1163.3	128	3.73	34.9
6	163.4	168.3	1162.0	128	4.01	34.9
7	175.6	180.2	1160.4	128	4.31	-34.9
8	188.7	193.0	1158.7	128	4.63	-34.9
9	202.8	206.8	1156.6	128	4.98	34.9
10	217.9	221.6	1154.2	128	5.35	34.9
11	234.2	237.7	1151.4	128	5.75	-34.9
12	251.7	254.9	1148.2	128	6.18	-34.9
13	270.6	273.5	1144.5	192	4.43	34.9
14	284.0	286.8	1141.7	192	4.65	34.9
15	298.2	300.8	1138.6	192	4.88	-34.9
16	313.0	315.5	1135.1	192	5.12	-34.9
17	328.6	331.0	1131.3	192	5.38	34.9
18	345.0	347.3	1127.1	192	5.65	34.9
19	362.2	364.3	1122.4	192	5.93	-34.9
20	380.3	382.2	1117.3	192	6.22	-34.9
21	399.2	401.1	1111.6	256	4.90	34.9
22	414.1	415.9	1106.9	256	5.08	34.9
23	429.6	431.3	1101.8	256	5.27	-34.9
24	445.6	447.3	1096.3	256	5.47	-34.9
25	462.3	463.9	1090.3	256	5.67	34.9
26	479.6	481.1	1083.9	256	5.89	34.9
27	497.5	498.9	1076.9	256	6.11	-34.9
28	516.1	517.4	1069.4	256	6.33	-34.9

Table 1. Stereo wire arrangement in the SWC (Part 1 of 2)

Nr.	Radius (z=0) (mm)	Radius (z=zm) (mm)	zm (Len/2) (mm)	Number of wires	Drift-dist. (mm)	Stereo angle (mrad)
29	535.4	536.6	1061.3	320	5.26	34.9
30	551.4	552.6	1054.2	320	5.41	34.9
31	567.8	569.0	1046.7	320	5.57	-34.9
32	584.8	585.9	1038.7	320	5.74	-34.9
33	602.3	603.4	1030.2	320	5.91	34.9
34	620.3	621.3	1021.0	320	6.09	34.9
35	638.9	639.8	1011.3	320	6.27	-34.9
36	658.0	658.9	1000.8	320	6.46	-34.9

Table 1. Stereo wire arrangement in the SWC (Part 2 of 2)

4.3 TRACK RECONSTRUCTION IN THE SWC

The new constraint obtained from the chosen stereo arrangement opens a rich arsenal of track reconstruction strategies, like:

1. Track finding in the +2° view by methods known from axial wires, and a 'traditional' computation of the z coordinates from the -2° view, plus straight line fits in in the r-z view, (more exactly the s-z view, with s the projected track length).

2. Same method starting from the -2° view.

3. Finding the projected tracks in both views, and matching them via the constraint of equal curvature.

4. Finding a track in the +2° view, and searching in the -2° view with preset curvature.

5. Same method starting from the -2° view.

Since high track densities produce occasional overlaps which cannot be resolved in one view (even with a larger number of samplings), the two independent reconstructions together with the strategies listed above provide the possibility to disentangle complicated topologies. As can be seen

from comparing the two event views in Figure 6 and Figure 7 on page 24, even the small difference in the stereo angle produces sizeable shifts of the overlap patterns, and helps to analyse closely spaced tracks in at least one view.

To obtain reliable results on the problems of pattern recognition, momentum resolution and track confusion a detailed Monte Carlo study has been performed which tracks the particles through the SWC as specified in Tbl. 1 (p.20) and Tbl. 2 , including the simulation of multiple scattering, particle decays, and field non-uniformities.

Measurement error on wire	$\sigma(r\varphi)$	= 150 μm
z-resolution (= $\sigma(r\varphi)/(\sqrt{2}\cdot\tan 2°)$	$\sigma(z)$	= 3.0 mm
Wire efficiency	η	= .98
Nominal magnetic field	B	= 1.3 T
Absorber Thickness (X_0 = radiation length)		
Beampipe	d	= 0.5% · X_0
Gas (1 bar)	d	= 0.5% · X_0
Wires (hexagonal cells)	d	= 1.2% · X_0
Total	d	= 2.2% · X_0

Table 2. Parameters of the SWC used for the Monte Carlo Simulation

As a first attempt, tracks were reconstructed in both stereo views by a program which was adapted from an axial wire geometry. The track efficiency was found high enough so that the views could be matched on the track basis (strategy 3) without the need to develop and tune other strategies at this stage. This track reconstruction program essentially has three important features:

- The patterns of the tracks are reconstructed within a single stereo projection. For simple events (collinear 2-prongs) the program finds on average 17.7 out of 18 possible coordinates per track independently of the momentum between 1 and 20 GeV.

- Since wrongly assigned drift ambiguities deteriorate the measurement of the particle momentum, angle etc., special attention is required to resolve them correctly. The proposed method which was tested in Monte Carlo and in real events from the new PLUTO central detector, consists of initially fitting circles to the positions of the struck sense wires, then to the drift isochrones by first preferring large (unambiguous) ones, and finally by weighting all drift information equally. Figure 9 on page 27 shows the inverse projected momentum corre-

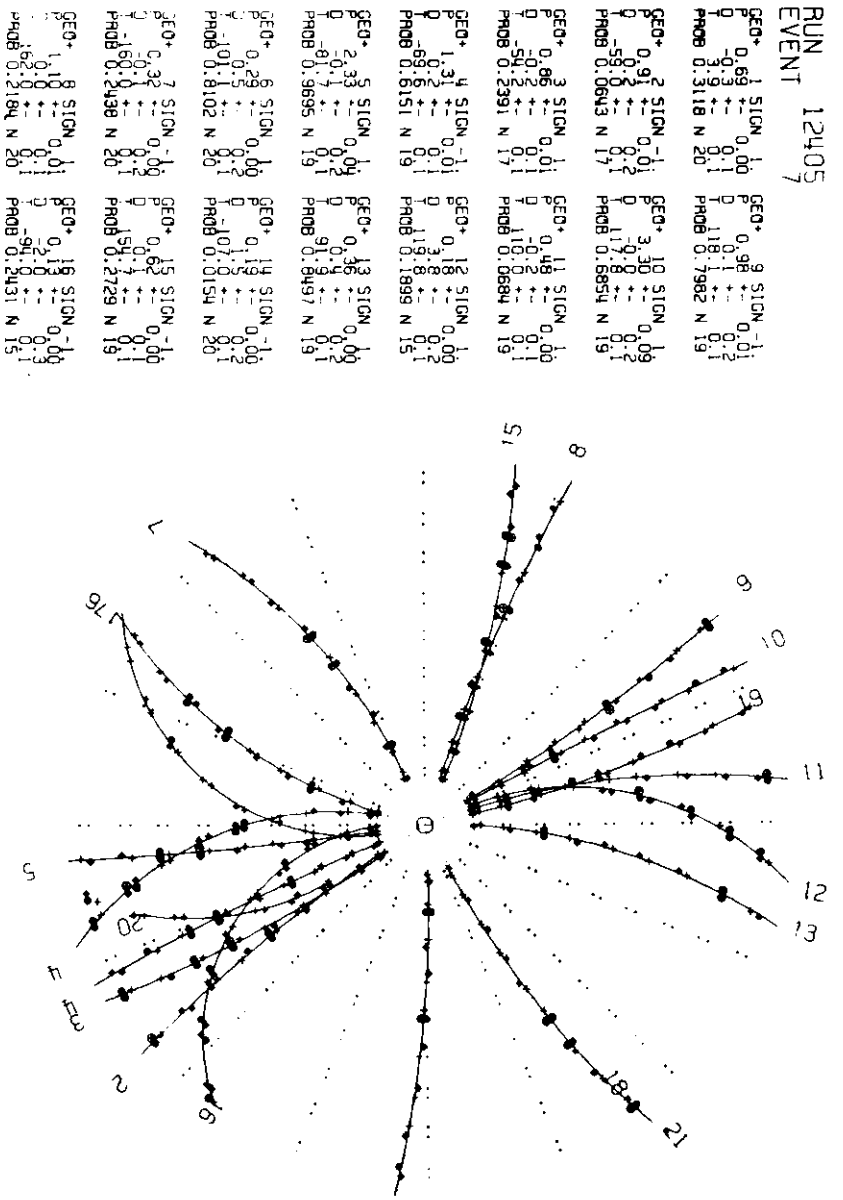

Figure 6. Multihadron event at $\sqrt{s}$ = 40 GeV, (+)-view

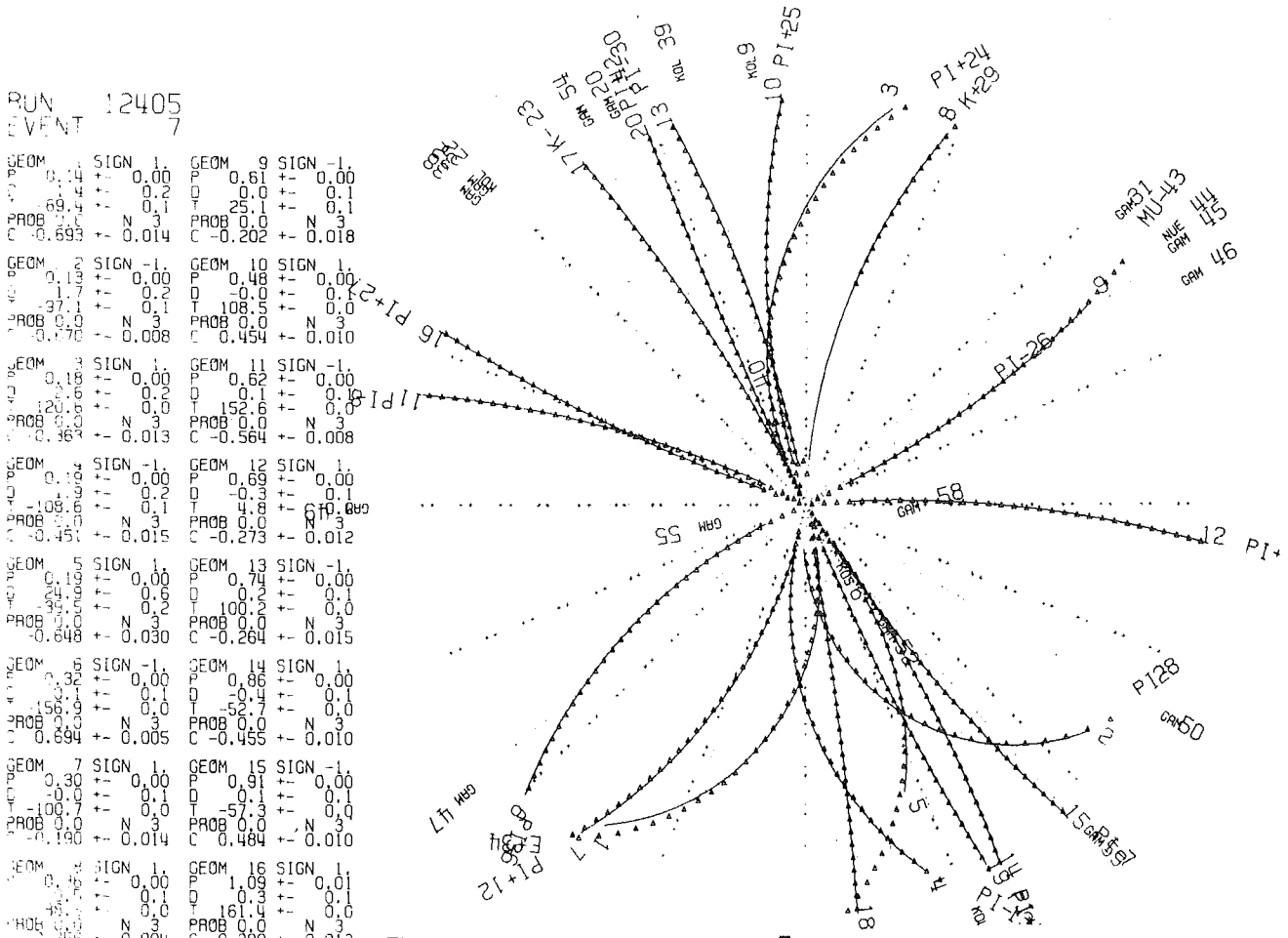

Figure 8. Multihadron event at $\sqrt{s}$ = 40 GeV: reconstructed r-φ-view (full line) and MC-generated tracks as seen in an ideal detector (triangles).

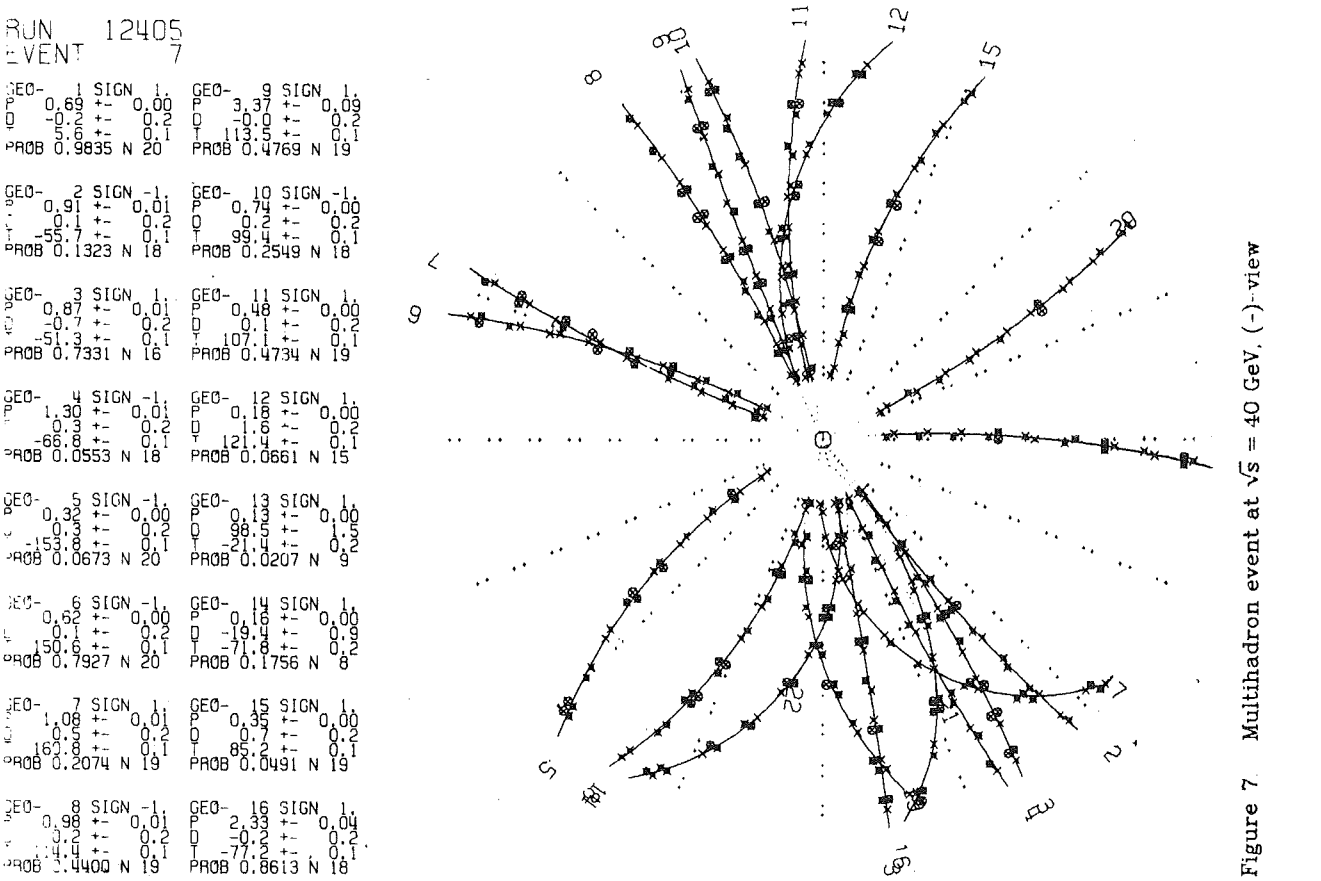

Figure 7 Multihadron event at $\sqrt{s}$ = 40 GeV, (-)-view

lation between both stero views for 1 GeV tracks showing a narrow band with almost no 'background'. Figure 10 on page 28 shows the vertex distribution of 20 GeV tracks. Also this plot has almost no background, and a vertex resolution of 0.12 mm is obtained which roughly corresponds to the resolution for the driftchambers used in the Monte Carlo simulation (Tbl. 2 (p.22)).

- A first order momentum fit is applied to the patterns in both stereo projections, and then both momenta are used for matching the projections.

With the track reconstruction developed so far we are able to reconstruct high multiplicity hadronic events (at $\sqrt{s}$ = 40 GeV). Figure 6 and Figure 7 on page 24 show the two stereo views of an event. Figure 8 shows the result of simply matching the tracks (strategy 3), without any attempt to improve the reconstruction by resorting to other strategies. The full lines represent the track parameters simply calculated as the averages of the stereo parameters. The comparison with the undisturbed Monte Carlo tracks (triangles) shows that the matching does work satisfactorily for this event (and others, too), but the calculation of the track parameters still needs some refinements.

In summary a Monte Carlo study of the proposed SWC yields momentum resolutions consistent with the predicted ones shown in Figure 11 on page 29.The predictions are given as a function of the polar angle ϑ for different momenta both with (a) and without (b) using the interaction point as an additional constraint. At ϑ = 90° a resolution $\sigma(p)/p^2$ = 0.005 GeV^{-1} is obtained. The resolution of the polar angle is $\sigma(\vartheta)$ = 4 mrad, the precision of the vertex is $\sigma(r_{min})$ = 120 μm.

4.4 CHARGE DIVISION

Track reconstruction in the SWC becomes impossible for tracks with polar angles $\vartheta \lesssim$ 200 mrad, where not enough wires have been set to make a fit and to resolve the drift ambiguities. Thus a direct z information on some of the innermost layers is needed. The resulting triple coordinates can be used as space points, but also be projected into any view in which they are needed for a track search. Using a vertex constraint or hits in the endcap proportional chambers this allows to measure tracks down to $\vartheta \sim$ 140 mrad. Direct z information on some layers distributed over the entire radius of the SWC also provides the possibility of an r-z-trigger.

Information on the z-coordinate can be obtained from individual wires by the charge division method, i.e. measuring the charge at both ends of a

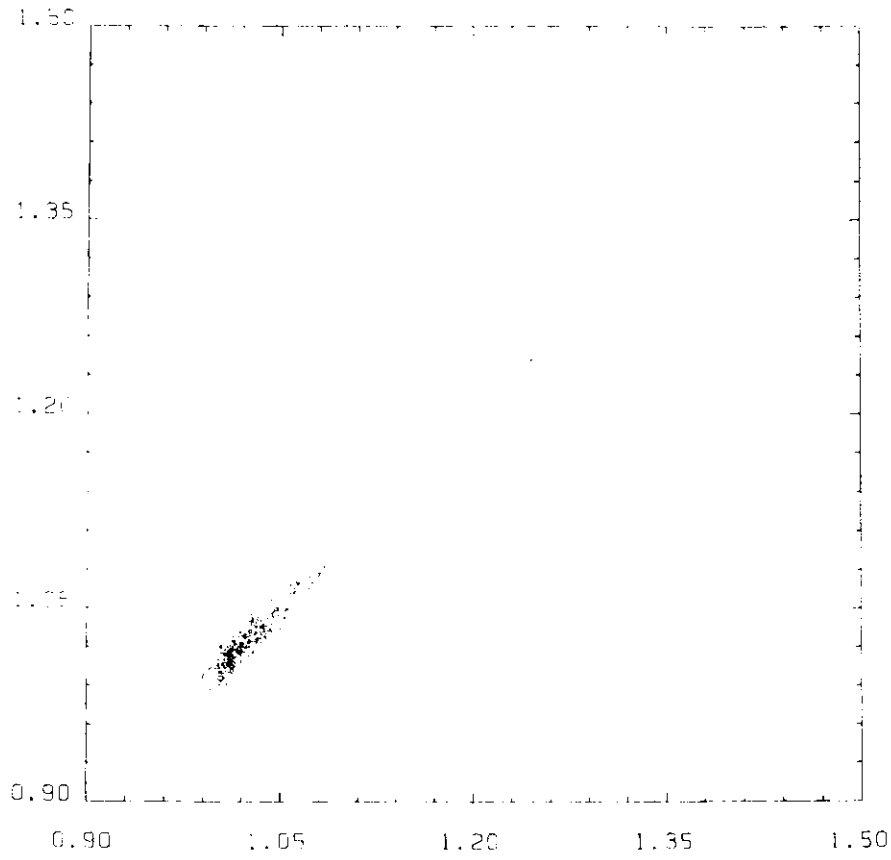

Figure 9. Correlation of the inverse projected momentum (1/p) (+)-view versus (-)-view, (1/p) in GeV^{-1}, ϑ > 30°

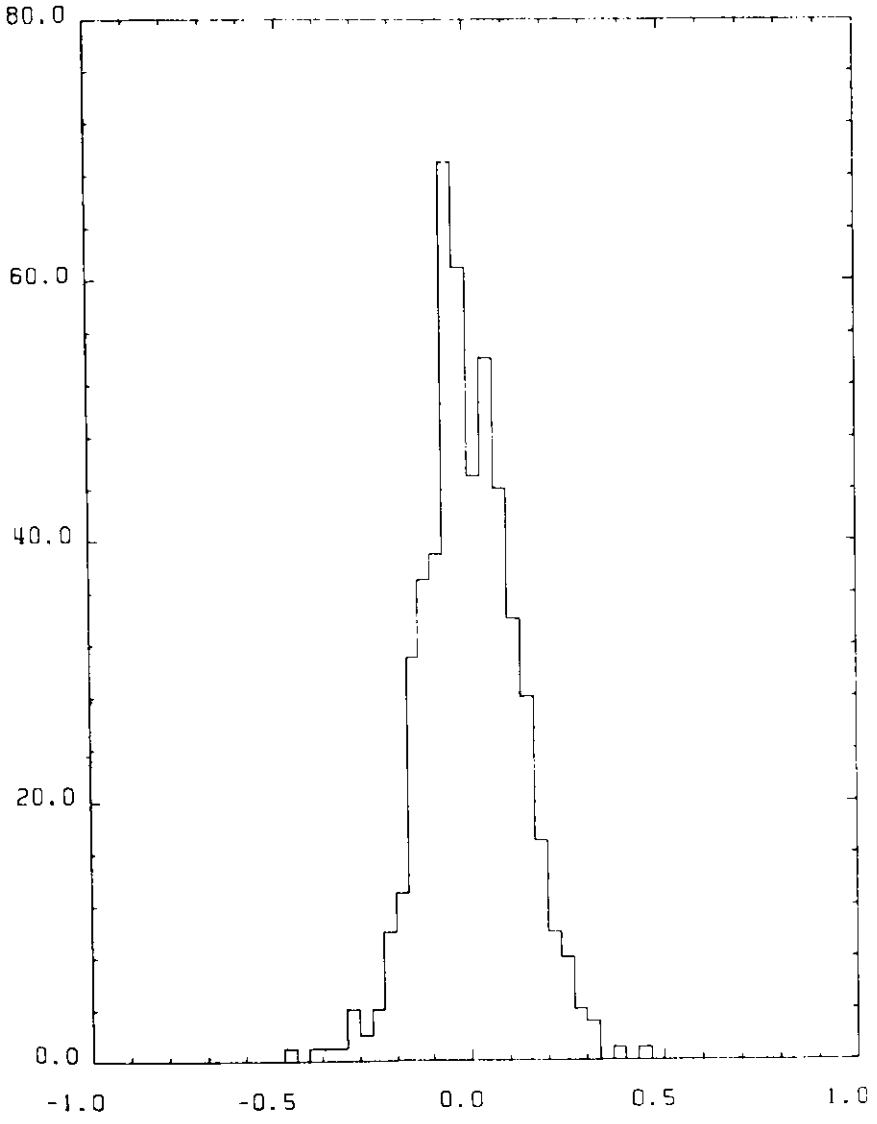

Figure 10 **Vertex distribution for 20 GeV particles: minimal distance to the interaction point in mm, averaged over both stereo views**

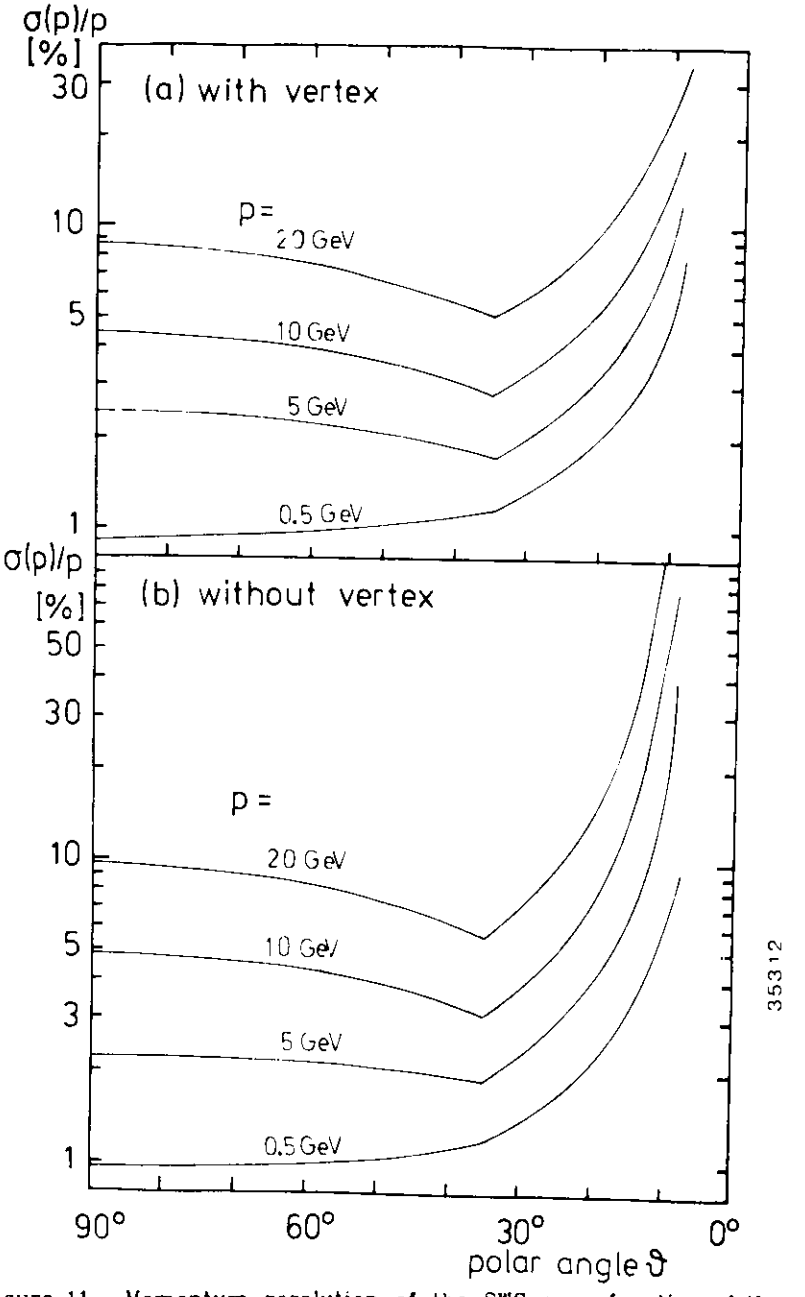

Figure 11. Momentum resolution of the SWC as a function of the polar angle: (a) with and (b) without using the interaction vertex as additional constraint.

wire with a low impedance amplifier. From existing detectors one can extrapolate that a z-resolution of $\sigma(z)/L = 1\%$ (L = length of the wire) can be achieved with this technique.

This z-resolution of the charge division information is sufficient to be used in the trigger and in track reconstruction. Once a track is found, a fit can be made using the information from the drift wires only. The precise z and ϑ information would therefore still be extracted from the stereo wires.

We intend to equip ~1750 wires with the necessary double ADC readout for charge division measurement. To be able to measure tracks down to small polar angles, we foresee to equip the innermost chambers 1 to 8, and, for the r-z-trigger, four further layers, namely chambers 12, 20, 28 and 36. These layers have radii similar to those of the proportional chambers of the present CELLO central detector which provide the r-z-trigger now.

We have the option to equip more layers just by adding more electronics without further modifications. The mechanical layout of the detector allows for double ADC readout on all wires.

4.5 PARTICLE IDENTIFICATION

It is obvious that particle identification over the full momentum range is a highly desirable feature of any future detector. But within the limited space in the CELLO coil, only a moderate particle identification of the charged particles is possible.

4.5.1 dE/dx-Measurement

In the proposed SWC, charged particle identification is possible by pulse height measurements on the wires. However, such measurements are inherently difficult in the presence of a high transverse magnetic field, because of the complicated curling drift trajectories. Changing to an octagonal or rectangular shape does not significantly simplify this drift behaviour at 1.3 T. All preamplifiers are designed so as to allow connection to a main amplifier of an ADC channel. On the assumption that all wires are equipped with an ADC readout and using the standard formulae /17/, the dE/dx resolution which could be obtained with this detector is between 7% and 10% in Argon (corresponding to about half these values in Propane). The figure of merit for particle identification is the number of standard deviations by which the ionisation loss curves for different particles are separated. In Figure 12 on page 31 we have plotted this value for K/π-separation (a) and π/e-separation (b) as a function of

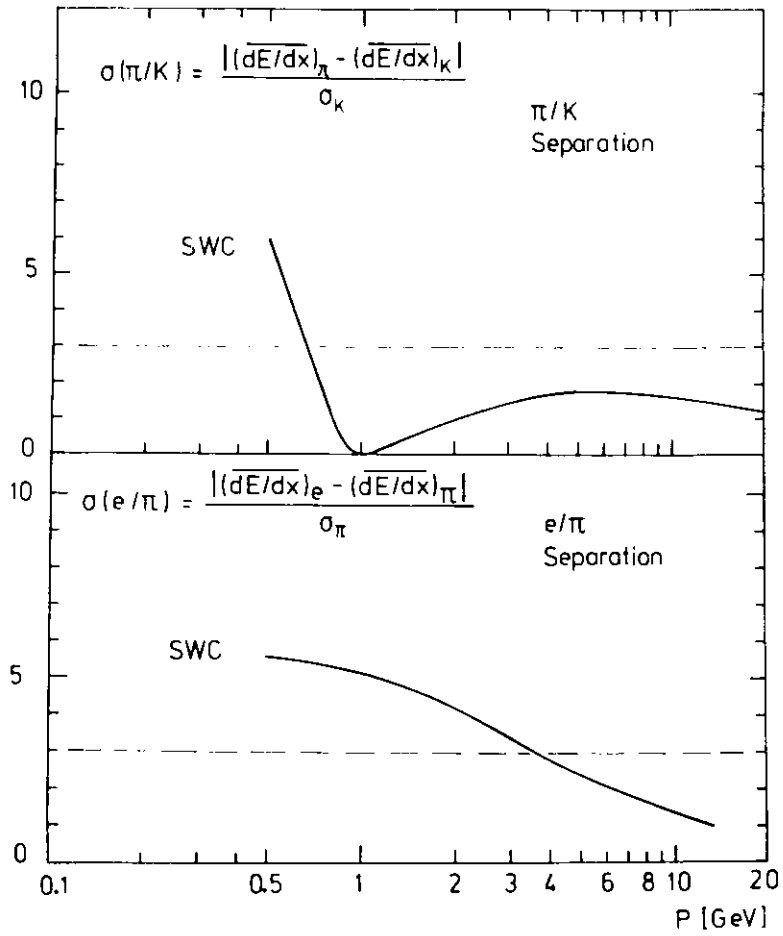

Figure 12 Particle separation in the SWC: assuming a dE/dx resolution of $\sigma/(dE/dx) = 9.5\ \%$ in Argon.

the particle momentum. Calling a difference of 3 σ a separation, K/π-separation is possible for momenta $\leq$ 650 MeV, while π/e-separation is possible up to ~ 3.5 GeV. It should be mentioned that in the region between 1 and 2 GeV the π/e-separation of the liquid argon calorimeter becomes fully effective, so that π/e-separation could be possible over the full momentum range.

It is not clear up to now whether this moderate particle identification can be achieved. From the experience of other detectors is seems to be non-trivial to obtain the ionisation loss from the pulse height measurement. In particular there are two special features of the proposed SWC which make this measurement even more complicated: (i) the small hexagonal drift cell with the high transverse magnetic field, and (ii) the variation of the shape of the individual cell with z. Measurements of the ARGUS collaboration indicate that the z-variations of the cell size does not introduce major problems. We plan to use the channels which are equipped with ADC readout anyway (for charge division measurement) to study these problems. Before the installation of the SWC the problem of the optimal evaluation of the pulseheights will be studied in a small test module. Additional information will also be available from the analysis of the test runs with the new PLUTO inner detector, which also has hexagonal cells.

4.5.2 Kinematic Reconstruction of Invariant Masses

Unstable particles are identified by reconstructing the invariant mass of their decay products. The precision of such a reconstruction depends on both the momentum resolution, and the angular resolution of the detector. For a particle of mass M decaying into two light particles of momenta p_1 and p_2 with opening angle α, the mass is

$$M = 2\sqrt{p_1}\sqrt{p_2} \cdot \sin(\alpha/2)$$

Taking $\sigma(p) = \kappa \cdot p^2$ ($\kappa \sim 0.005$ GeV^{-2}, the momentum resolution of the SWC) one obtains

$$(\sigma(M)/M)^2 = \{\kappa^2 \cdot (p_1/p_2 + p_2/p_1) + [2\sigma(\alpha)\cdot\cos(\alpha/2)/M]^2\} \cdot p_1p_2/4$$

With the proposed stereo angle of 2° the mass resolution at 1.6 GeV has equal contributions from momentum and z resolution. Down to all but the lowest polar angles the K^0 mass resolution is dominated by the z-resolution $\sigma(\vartheta)$:

$$\sigma(M_K) \sim \sqrt{2}\, p_K\, \sigma(\vartheta) = 0.006\, p_K.$$

4.6 TRACK TRIGGERS

The SWC described above fits well into the present CELLO track trigger philosophy which is based on the general recognition of two tracks. Only minor modifications have to be made to the existing system. In the following section the impact of the SWC on the trigger is discussed for the different trigger-'components' involved.

r-φ Trigger

It is possible to connect the present CELLO trigger to one of the stereo views. Since the tracks have practically the same curvature as in an axial view, the momentum cut-off will not be changed if similar radii for the triggering layers are chosen. The arrangement of having a large number of layers in sets of four, each set having two layers with +2° followed by two layers with -2° stereo angle, allows an interesting improvement: One can derive the input signals from an OR of two neighbouring layers, which is to leading order fully efficient, and operate the trigger with higher redundancy, e.g. 7 out of 7 ORs instead of the present 5 out of 7 layers.

r-φ-Endcap Trigger

For polar angles < 30° a trigger which combines r-φ signals with those of the endcap proportional chambers (ECPC) has proved to be extremely useful. In order to conserve this feature, either we change the trigger logic or we modify the cathode plates of the ECPC. In the latter case the endcap φ-segments have to form a natural extension of the triggering stereo view. This means that every line which separates two φ-pads will have to be moved sideways by z·tan 2° = 49.1 mm for the first and 49.8 mm for the second chamber. The whole cathode then looks like shown in Figure 13 on page 34.

r-z Trigger

Although basically the z-information for the trigger could be extracted from the stereo views in the same way as done for the spatial track reconstruction, it appears more practical to use some layers with charge division (see Sec."Charge Division" on page 26) and obtain z-signals within 1 μsec. The electronics for an analogue conversion of the current into z-signals, and for storing them in the appropriate registers is under study.

r-z-Endcap Trigger

The combination of the r-z- with the ECPC-signals is straightforward. One only has to modify the mutual assignment, that is to combine the

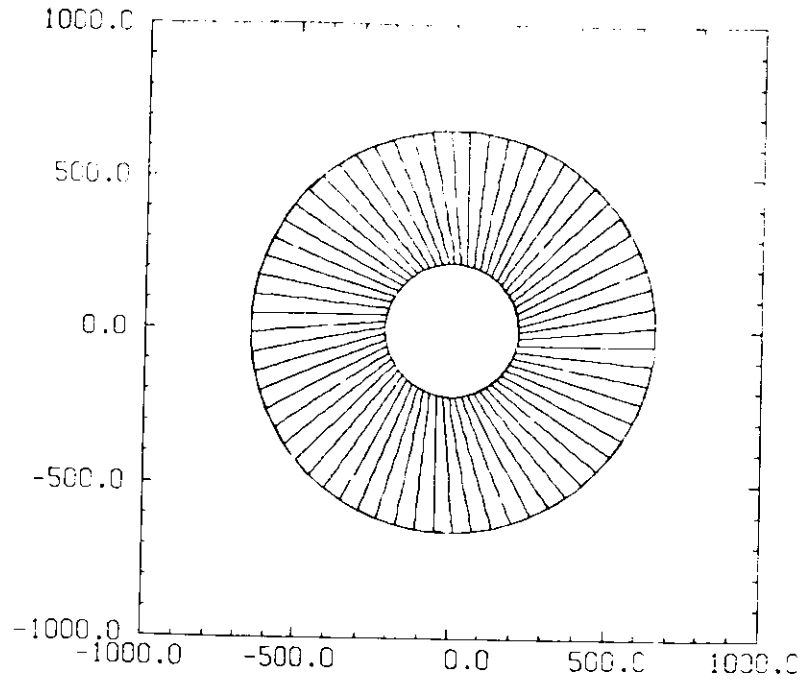

Figure 13. Segmentation of ECPC cathodes

z-signals corresponding to stereo wire radius r_0 (at z=0) with an endcap pad radius which has $z \cdot \tan\alpha \sim 49$ mm added in quadrature to r_0.

4.7 READOUT ELECTRONICS OF THE SWC

The ster o wires are either read at one side only, or if charge division is requested. on both ends. Newly developed preamplifiers will be installed which can be used simultanously for an ADC and a TDC readout. Thus one end of the wire is connected with at most one signal cable to the electronics racks.

The possible configurations of electronic read out are listed in Tbl. 3 together with their prices (status of Febr. 1983). The colums refer to the following configurations: complete readout on both ends (1), complete readout on one end (2), and TDC readout only on one end (3)

The best solution for the TDC and ADC channels would certainly be a complete new design, including new features like self-calibration of the

system, instead of the present 'manual' adjustment procedures, and large scale integration (e.g. up to 96 channels/card). At the PLUTO detector many TDCs of relatively new design are available. We intend to use those which have been purchased by Glasgow University in this experiment. Within the limited budget available during the construction of the detector, we shall try to keep as many options open as possible and start with a minimal solution for the electronics which could easily be upgraded afterwards. As a minimal solution we consider equipping all wires with TDC readout only and ~ 1750 wires with additional double ADC readout.

Configuration Nr. / Item	1	2	3	Price DM
Preamplifier	2	1	1	30
Cable	2	1	1	50
ADC channel	2	1	0	150
TDC channel	1	1	1	150
Adapter (TDC and ADC on same end of wire)	1	1	0	30
Price of configuration	640	410	230	DM

Table 3. Electronic equipment for SWC wires

5.0 FORWARD TAGGING COUNTERS

The angular region accessible to the forward taggers ranges from 26 to 110 mrad. The adjacent endcap calorimeter becomes efficient for angles ϑ > 140 mrad. As explained under "Specification of the New Detector Components" on page 14 we have to choose a two step solution consisting of a large angle forward detector (LAF) covering the range 50 < ϑ < 110 mrad and a small angle forward detector (SAF) covering the range 26 < ϑ < 50 mrad. Each detector consists of a shower counter and 4 planes of tube chambers for e/γ separation. Figure 14 on page 37 shows the proposed setup of the forward detectors.

5.1 LARGE ANGLE FORWARD DETECTOR (LAF)

5.1.1 BGO Shower Counter

The design of the LAF shower counter has to cope with a number of extremely difficult conditions:

- The counter is exposed to a field of 0.5 to 1 T.
- The available space is limited by the presence of pumps and tube chambers to a length of ~ 350 mm including readout. The free space in the radial direction is only 100 mm.

We propose using an array of bismuth germanate (BGO) crystals as a shower counter. BGO is the only material known to us, which meets the above topological conditions and yet yields an adequate resolution, matching the resolution of the endcap counters. In particular, BGO has the following favorable properties:

- short radiation length of 1.12 cm (This allows a good longitudinal containment in the proposed 20 cm long volume. It also optimizes the lateral containment. In BGO 50 % of the shower energy is contained within a cylinder of 5 mm radius),
- potential for photodiode readout, which works in the fringe field (The low noise preamplifiers can be mounted directly behind the photodiode),
- radiation resistance,
- easy segmentation for measuring the position of photon showers.

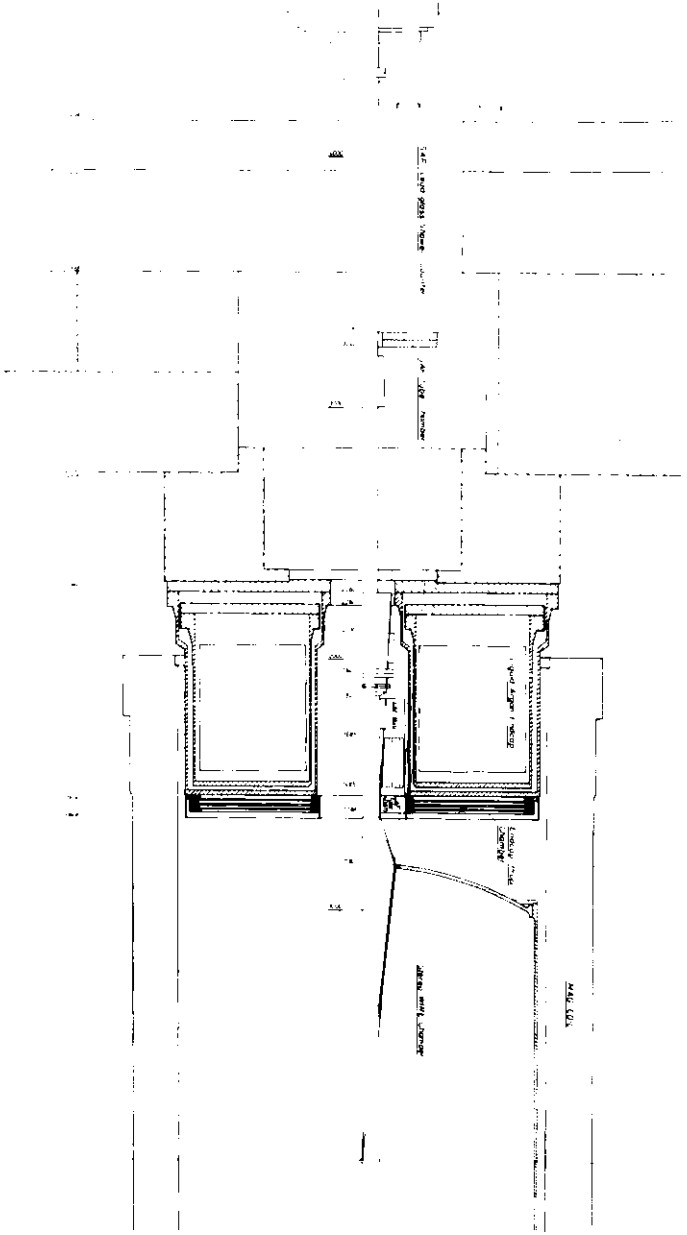

Figure 14. General view of the CELLO forward region

Figure 15 shows a side view (vertical cut) of the array, and Figure 16 on page 39 shows a front view. The array consists of 6 rings of crystals. The rings are divided azimuthally in segments of 6.9° width. The crystals have trapezoidal cross sections and a length of 20 cm. This corresponds to 17.9 radiation lengths. The segmentation is optimized to match the size of commercially available photodiodes which are used to read out the crystals. The total number of crystals and electronic channels is 632. The crossed parts between R7 and R8 indicate the areas missing at the rear of the crystals due to the conical shape of the inner edge.

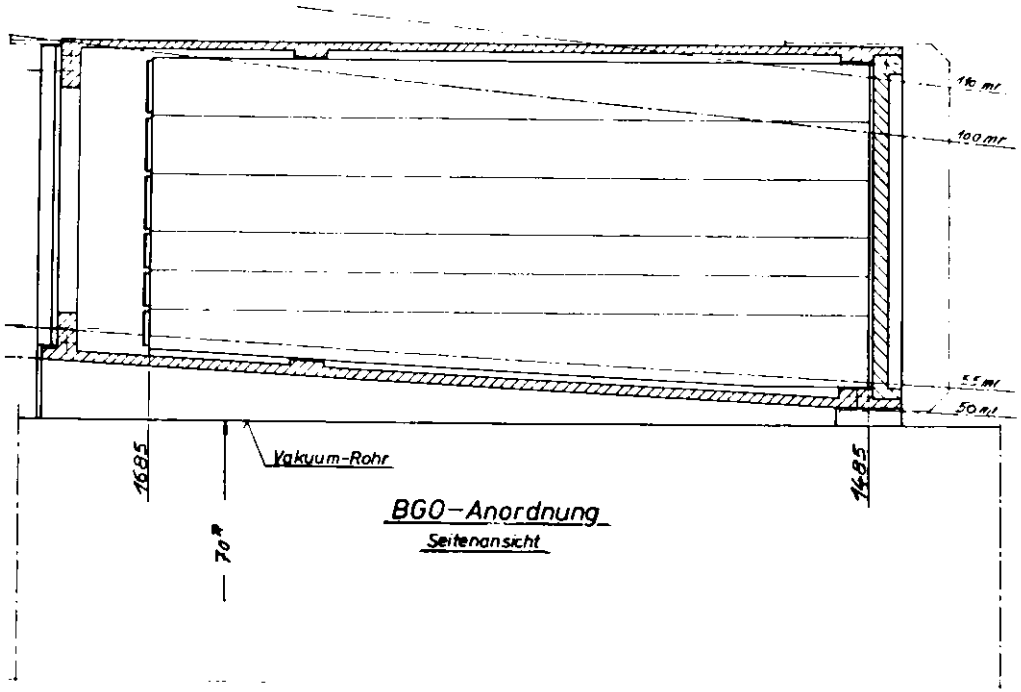

Figure 15. Side view of the BGO array (vetical cut)

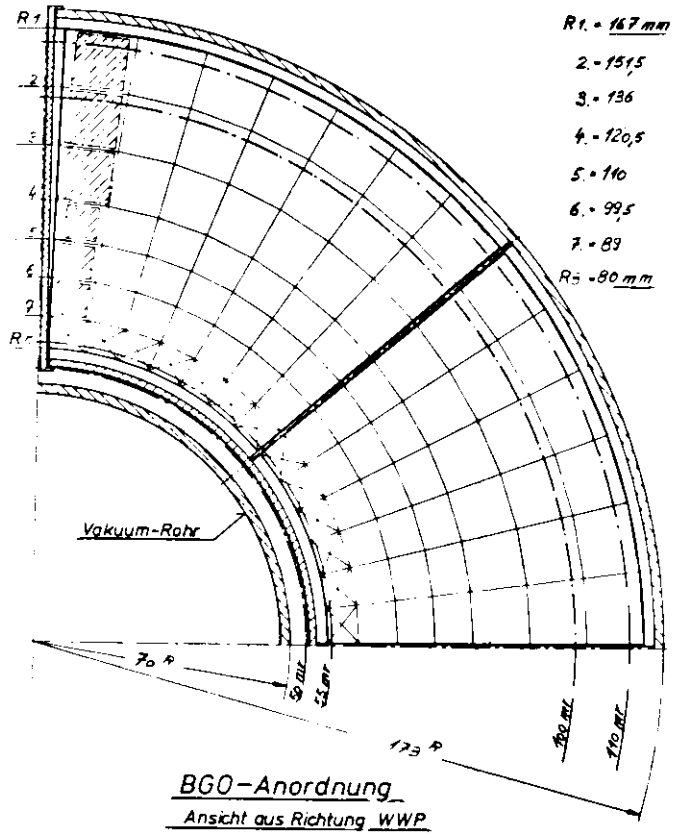

Figure 16 Front view of the BGO array of the LAF The shaded areas indicate the size of photodiodes

The crystals will be mounted in a water cooled container, which will be temperature stabilized to 0.5°C. The inner wall of the container is conical and leaves the 50 mrad cone free of material. The inner edge of the crystals is at 54 mrad. The effective region of the counter where more than 50% of the shower energy is contained ranges from 56 to 106 mrad. Leakage losses of electron showers at the edges will be partially corrected for, using known shower profiles and the space information from the LAF tube chamber (see "Drift Tube Detector" on page 41).

The counter provides very good spatial resolution ($\sigma \sim 2$ - 3 mm for shower energies > 1 GeV /18/). The energy resolution $\sigma(E)/E$ will be on the 3% level above 1 GeV. It is limited by transverse leakage. Recently the energy resolution of BGO crystals with photodiode readout has been measured. A resolution of $\sigma(E)/E = 3\%$ in an array sized $6 \cdot 6 \cdot 20$ cm^3 at 4 GeV has been obtained from a first analysis /19/. These results are confirmed by tests performed at DESY. Due to the small radiation length of 1.1 cm the transverse leakage of BGO is smaller than in typical scintillator sandwich counters like the PLUTO small angle tagger (SAT), which has an effective radiation length of 1.72 cm. Good lateral containment of the shower is important in view of the limited lateral extension of the counter. The Q^2 resolution of the tagged electrons will be $\sigma(Q^2)/Q^2 \sim 6\%$. This is comparable to the resolution of the liquid argon endcap counters. Equally important, the BGO counter in conjunction with the the LAF tube chambers will resolve the shower positions of photons from 1γ- and 2γ-reactions with typical resolutions of $\sigma(\vartheta) \approx 3$ - 4 mrad and $\sigma(\varphi) = 30$ mrad. In addition relativistic charged pions can be located in the BGO from their energy deposit of 180 MeV.

From present experience we expect that the proposed counter will function adequately in the radiation enviroment of PETRA. M. Kobayashi et al./20/. have demonstrated that BGO of 99.999% purity has more than 100 times higher resistance against low energy photon radiation than SF5 lead glass. Most of the observed radiation damage due to photons recovers by itself after several hours. These findings have been confirmed recently by radiation tests at DESY /21/. A qualitative check of the radiation resistance of crystals exposed on the PLUTO and on the CELLO beam pipe has shown no damage. Both the LAF shower counters and tube chambers will be shielded by 1 mm of lead against scattered sychrotron radiation.

Each segment of the BGO shower counter array is read out by a silicon photodiode attached to its end. The photodiodes work well in magnetic fields. The pulse readout system will consist of low noise preamplifiers developped at the Max-Planck-Institut in Munich. The preamplifier and shaping amplifier will be mounted as a hybridized chip behind the BGO crystals. The signal then will be fed to a standard ADC.

The combination of photodiodes and low noise amplifiers has a gain stability of better than 1% /19/. Gain variations due to temperature changes of the BGO will be kept below 0.5% by using a water cooled insulated container. Calibration and stability monitoring will be done using events from Bhabha scattering and cosmic ray signals. A cosmic ray muon deposits about 14 MeV in a 1.5 cm thick BGO crystal at perpendicular passage. Signals of this magnitiude can be well separated from noise when using low noise photodiodes like the Hamamatsu S1723.

The status and the time schedule of the project is the following:

A matrix of 38 crystals ($1 \cdot 1 \cdot 15$ cm^3) has been tested in an electron beam at DESY during December 1982. The readout consisted of Hamamatsu S1337 photodiodes together with preamplifiers developped at DESY for liquid argon counters. The analysis is underway. Further tests will be carried out in the first half of 1983 using improved photodiodes (Hamamatsu S1723) and improved preamplifiers. Design studies for a water-cooled container have started.

We anticipate acquiring part of the necessary amount of BGO during this year for additional tests and the rest in 1984. Hence the full array can be mounted together with the LAF tube chambers late in 1984 in connection with a modified beam pipe (see "Beampipe" on page 49).

5.1.2 Drift Tube Detector

The tube chambers in front of the BGO shower counter have to serve two purposes:

- provide an accurate r and φ measurement of the point of passage of charged tracks,
- allow e/γ identification in conjunction with the signal from the BGO counter.

The accurate r information of $\sigma(r) = 1$ mm or better is necessary particularly at the edges of the BGO counter in order to determine the fraction of leakage energy. It also helps for cross checks and calibration. Further design criteria are (i) minimizing the amount of material in the chambers and (ii) providing a sufficient number of layers in order to reduce the confusion caused by spurious hits from soft photons. On the other hand from a logistic point of view the number of electronic channels should be kept as low as possible.

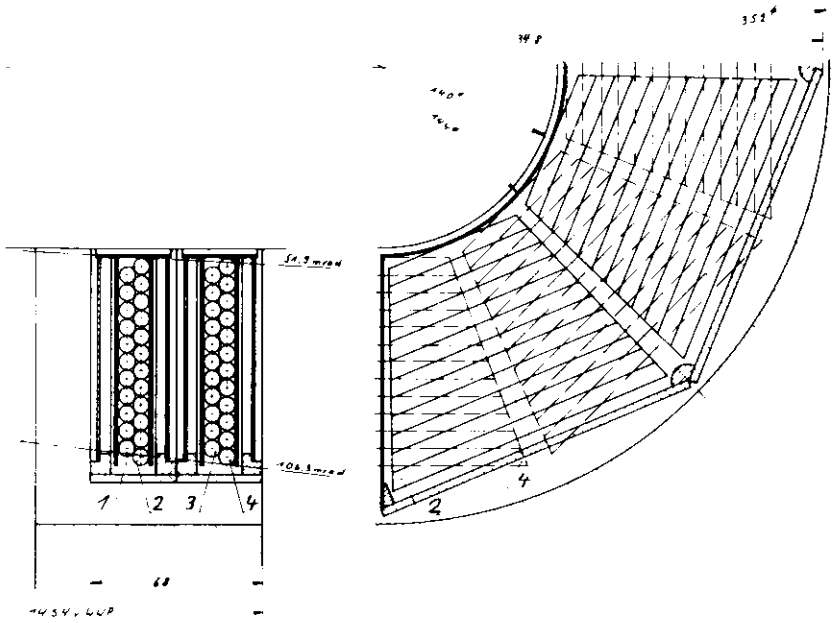

Figure 17. The LAF drift tube chamber

We propose a solution of drift tube chambers similar to the present beampipe detector of CELLO. Figure 17 shows a front view and a side view of one quarter chamber. The detector consists of two double layers of aluminum tubes (wall thickness 0.2 mm). The tube diameter is 6.6 mm. Each double layer is subdivided azimuthally into 8 segments of 45° width. The rear double layer (layers 3 and 4 in Figure 17) is rotated by $\Delta\varphi = 22.5°$ with respect to the front double layer (layers 1 and 2). This leads to a complete azimuthal coverage for polar angles of $53 < \vartheta < 106$ mrad (requiring at least one double layer to be hit).

The tubes will be read out by preamplifiers and TDCs of the same type as used in the PLUTO experiment (a total of 768 channels). The radial position resolution will be better than 0.5 mm and the azimuthal resolution between 10 and 20 mrad. The potential for identifying photon-initiated showers will depend largely on the amount of material in front of the chambers.

5.2 SMALL ANGLE FORWARD DETECTOR (SAF)

The small angle detector will consist of an existing shower counter and 2 - 4 planes of proportional tube chambers. The detector serves three purposes:

- monitoring of Bhabha events,
- tagging of electrons from 2γ-events,
- vetoing against hard photons from radiative 1γ-annihilation which could simulate an electron tag.

We consider two options for the shower counter: (i) the CELLO lead glass counter (FWD3) and (ii) the PLUTO small angle tagger (SAT).

5.2.1 The CELLO Lead Glass Counter

The forward lead glass detector currently in use at CELLO in the range of 50 to 110 mrad could be used as a SAF after some modifications and improvements. It would cover the range of 26 to 50 mrad. At larger angles it would be shadowed by the LAF.

The decrease of the minimum angle to 26 mrad can be obtained by moving the FWD3 from $|z| = 2650$ mm to $|z| = 3350$ mm and making the following modifications:

1. the inner edge of the lead glass blocks will be shaped in order to locate them as close as possible to the beampipe,

2. new stripes of circular scintillators will be added (see Figure 18 on page 45).

In addition some other improvements can be made to the FWD3. The position is determined by calculating the barycentre of the shower in the circular scintillators. The shower is obtained at present by the conversion of the electron (or photon) in the material in front of the FWD3 to which about one radiation length of lead is added. In the future the only material in front of the SAF will be the beampipe ($\lesssim$ 0.85 rad.length). The conversion will be obtained by adding lead glass blocks of 3 rad. length in front of the scintillators to provide an active converter.

As in the current design, we will put acceptance and luminosity counters in front of the lead glass converter. The performance of the modified FWD3 will be the following:

Total length = 17 rad. length
Acceptance : $26 < \vartheta < 50$ mrad
$\Delta\varphi \geq 3\cdot\frac{\pi}{2}$

Resolution : $\sigma(E)/E = (2 + 7/\sqrt{E})\%$
$\sigma(r) = 4$ mm
$\sigma(\varphi) \leq 10°$

The efficiency of the position measurement and of the e/γ-separation will be improved by adding tube chambers in front of the FWD3 (see below).

A problem which could affect the FWD3 is the radiation damage induced in the lead glass. In order to minimise such effects we leave space around the beampipe for 1.5 cm of lead shielding. We intend to put a lead glass block in the possible future position of the SAF in order to determine if the effect of radiation damage (yellowing of the lead glass) is still important.

If there are still serious problems of this type, the existing PLUTO SAT can be used to cover the 29 to 50 mrad region.

5.2.2 The PLUTO Small Angle Tagger

This sandwich counter contains 30 lead plates ot 3.4 mm thickness and 31 scintillator plates of 6 mm thickness. The counter is divided into 12 seg-

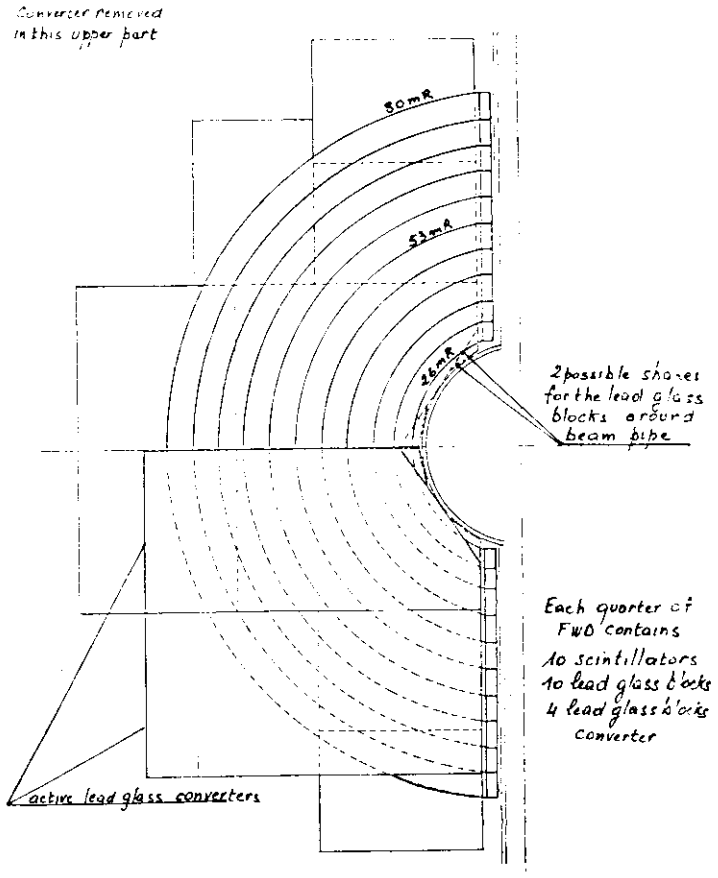

Figure 18. Front view of the small angle forward detector (SAF), option 1: modified FWD3, currently used at CELLO.

ments of $\Delta\varphi = 30°$. Each segment is read out by wavelength shifters at the inner and outer edge to allow a radial position measurement of showers by comparing the two pulse heights. Similarly a φ-position is obtained by comparing the pulse heigths from neighbouring φ-segments Figure 19 on page 47 shows a front view of the detector.

At the position |z| = 3700 mm the detector will cover the polar angle range from $29 < \vartheta < 70$ mrad. For $\vartheta > 50$ mrad the SAF is shadowed by the LAF.

In the PLUTO experiment the detector was installed at |z| = 3600 mm. Its performance for detecting high energy electrons was as follows:

Total length = 18.2 rad. length
Acceptance : $29 < \vartheta < 50$ mrad
$\Delta\varphi \sim 2\pi$

Resolution : $\sigma(E)/E = (17/\sqrt{E})\%$
$\sigma(r) = 7$ mm
$\sigma(\varphi) = 25$ mrad (with an efficiency of ~ 95%)

5.2.3 SAF Tube Chambers

We propose to install the existing proportional tube chambers which were attached to the PLUTO SAT. The tube chambers consist of 72 horizontal and 132 vertical brass tubes (cross section 10 · 10 mm², wall thickness 0.3mm). Two horizontal stripes at $60 < y < 80$ mm and at $-80 < y < 60$ mm are not covered by the tubes, corresponding to ~ 5% of the azimuthal acceptance of the SAT. The outer dimensions of the chambers are indicated as dash-dotted lines in Figure 19 on page 47. We have an option of adding two more planes of identical chambers. These will be oriented at 45° relative to the chambers shown.

In the PLUTO experiment the front of the chambers was shielded by 2 mm of lead (~ 0.35 rad. length). By requiring clean position information in the chambers electrons could be located with 85% efficiency, whereas only 10% of high energy photons simulated a clean electron signal. By combining the shower counter and the tube chamber information, photon initiated showers have been identified with ~ 65% efficiency.

We plan to improve these values by reducing thickness of the lead shield and adding two additional layers of tubes. Monte Carlo studies of a similar tube system /22/ show that most of the spurious hits accompanying the trajectory of an electron are caused by soft photons from two sources: (i) radiation in the material in front of the chamber, and

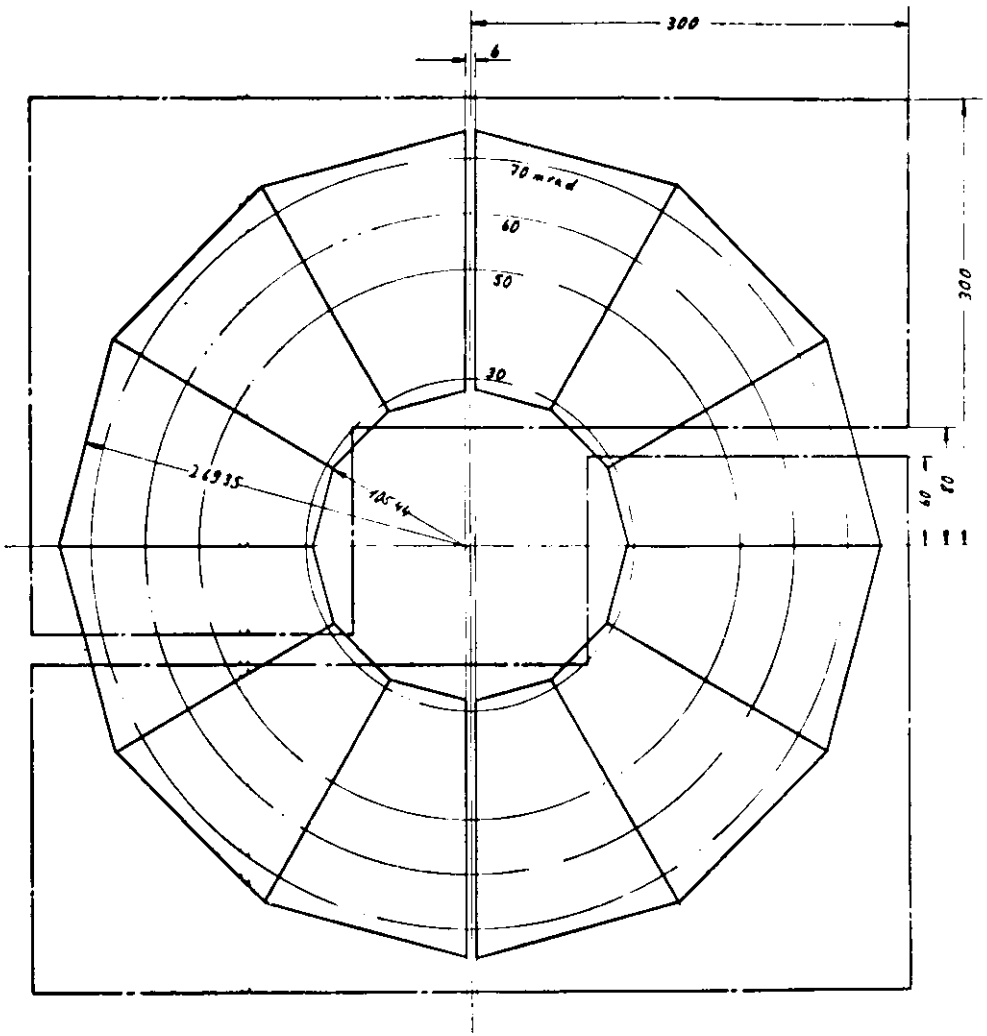

Figure 19. Front view of the small angle forward detector (SAF), option 2: PLUTO small angle tagger SAT. Full lines: boundaries of the lead scintillator sandwich, dash-dotted lines: boundaries of the two planes of horizontal and vertical proportional tube chambers

(ii) backscattering from the shower counter behind the tube chambers. The ambiguities caused by spurious single hits can be reduced by increasing the number of layers. Photon identification will be possible in the range of $26 < \vartheta < 39$ mrad.

6.0 BEAMPIPE

Here we first discuss the beampipe which will be used when all the items of this proposal are realised (so called "85-beampipe"). In the time before when already the LAF will be ready, an intermediate version of the beampipe ("84-beampipe") will be used, which is described at the end of this section.

6.1 85-BEAMPIPE

The beampipe in the experimental area ($|z| < 4320$mm) consists out of 3 mechanically separated parts:

1. the central section $|z| < 1900$ mm
2. two end sections with $1900 < |z| < 4300$ mm

A cross section of the beampipe is given in Figure 20 on page 50.

Each section will be equipped with sets of NEG pumps at $|z| \approx 2000$ mm and at $|z| \approx 3500$ mm to guarantee good vacuum conditions at the interaction region.

6.1.1 Central Section

The central section has a total length of 3800 mm. It can be easily transported and inserted into the SWC in the CELLO hall. It consists of five parts which are welded together and cannot be separated for mounting. The parts are: the inner pipe, two LAF windows and the first halves of two SAF trumpets.

- Inner pipe:

  This part is made out of beryllium. It has a length of 1100 mm, an outer diameter of 140 mm. The wall thickness is 1.5 mm (0.5% rad. length). This allows all particles with polar angles $\gtrsim 130$ mrad to enter the SWC with a minumum of multiple scattering. This thin beampipe is essential for the good vertex reconstruction capability of the SWC.

- LAF window:

  The polar angle region $110 < \vartheta < 130$ mrad is covered by the flanges of the liquid argon endcap calorimenter. Thus no particle detection is possible in this range. We use this range for a massive beampipe

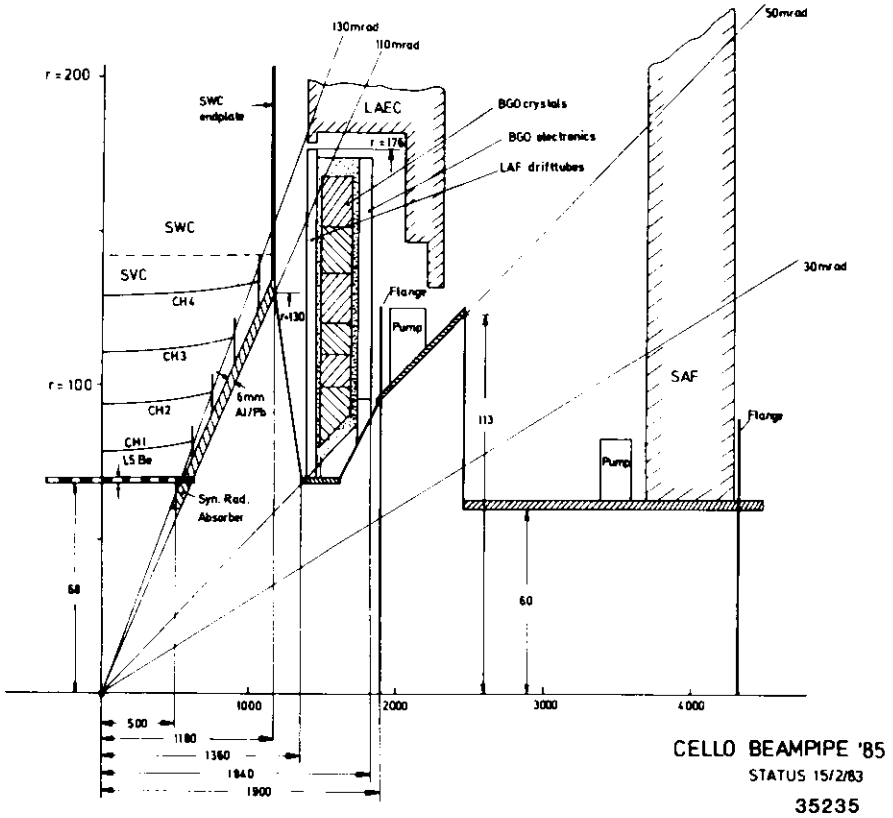

Figure 20. Cross section of the 85-beampipe: the scale on the r-axis is enlaged by a factor of 20 compared to the z-(=beam)-axis

trumpet which starts at |z| = 550 mm with a radius of 68 mm and ends at |z|= 1180 mm with a radius of 130 mm. The massive trumpet is a sandwich, made from aluminum and lead (in total 4 mm of Al and 2 mm of Pb) which has two main purposes: (i) to serve as end flange for the stereo vertex chamber and (ii) to protect the central detector against synchrotron radiation comming from the mini beta quadrupole. In the range 1180 < |z| < 1360 mm a thin (~2 mm Al) conical shaped window for the LAF covers the polar angle 50 < ϑ < 110 mrad.

- SAF trumpet:

  This section stats at |z|=1360 mm with a radius of 68 mm and ends in a flange at |z| = 1900 mm with an inner radius of 95 mm. Inside the LAF cooling pipes and 5 mm of thermal insulation will be mounted between the beampipe and the BGO container.

The central section will be equipped with a synchrotron radiation absorber, positioned at the end of inner pipe to shield the central detector. It covers the polar angle in the range 110 < ϑ < 140 mrad, the region of inefficiency between the LAF and the liquid argon endcaps. Further downstream, masks in the beampipe are foreseen to reduce the background. Details will be fixed later, after the PETRA quadrupole configuration is fixed and after our experience with the setup running this year has been evaluated.

6.1.2 End Sections

The end sections terminate the part of the beampipe of increasing diameter, making a vertical window for the SAF. This window is situated at |z| = 2260 mm between r = 60 mm and r = 123 mm, and has a thickness of 2 mm of aluminum. It will be traversed by particles in the polar angle range of 26 < ϑ < 50 mrad, which will be detected in the SAF. From the window to the end flange at |z| = 4320 mm the beampipe is a straight tube with an inner diameter of 120 mm. Additional absobers can be inserted here. The total length of each section is 2.42 m.

6.2 84-BEAMPIPE

At the end of 1984 the BGO for the LAF will be available. It is envisaged to use the LAF containers in the CELLO detector setup already at that time.

This implies some modification of the existing (83-beampipe) in the range $1100 < |z| < 1800$ mm to provide a window for the LAF. During this time the FWD3 detector will remain at its present place.

7.0 DATA ACQUISITION AND COMPUTER REQUIREMENTS

In principle the new components fit perfectly into the existing CELLO data acquisition scheme. Since the number of electronics channels is not greatly changed, the existing online computer capacity will be sufficient.

Details concerning the load on the online computer caused by the proposed items have not yet been worked out in detail. Especially the impact of the IBM-370-E emulator which will be provided by the Tel-Aviv group and which will be operative at the start-up of the SWC needs further studies.

The load on the offline computers due to data filtering, reduction, reconstruction and analysis is expected to be equivalent to our previous experiments. The computing capacity in the external laboratories and the equivalent contingency at DESY are therefore adequate.

8.0 COSTS, TIME SCHEDULE

The costs and the time estimates are given on the basis of the prices and the technical knowledge of Februray 1983.

8.1 COSTS

8.1.1 Investment Money

The investment money for the three proposed new components is listed in the tables below. They include only external costs. External manpower is assumed (partly) for stringing the wires and installation of the SWC.

Central Detector

The costs are specified in Tbl. 4 (p.55) . As pointed out in "Readout Electronics of the SWC" on page 34 we intend to equip ~1750 wires with type 1 electronics and the rest of ~5750 wires with type 3 electronics (see Tbl. 3 (p.35)). The prices for these channels (complete readout from preamplifier to online computer) are DM 640 and DM 230 respectively. Thus the total price for the readout electronics would be 2445 kDM. Using the existing TDC channels which have an equivalent value of ~465 kDM, the investment necessary for the readout electronics is 1980 kDM.

Forward Detectors

The costs of the forward detectors are specified in Tbl. 5 (p.56) . It includes the complete construction of the LAF using some cables and preamplifiers from PLUTO for the readout electronics. The costs of the modifications of the SAF are estimated on the basis of the modification of the present FWD3 detector.

Beampipe

The costs of the beampipe specified in Tbl. 6 (p.56) . Since the LAF will be already installed in 1984, modifications of the present beampipe are necessary (1984 beampipe). In the final setup a complete new construction is foreseen. It should be mentioned here again that the inner section (Pos. 2.1 and 2.2 in Tbl. 6) of this beampipe is an integral part together with the SVC (Pos. 1.2 in Tbl. 4 (p.55)).

	kDM
1. Mechanics and Gas supply	
1.1 Endplates	350
1.2 Vertex detector (without beampipe)	80
1.3 Outer cylinder	70
1.4 Wire feed-throughs (endplate)	200
1.5 Supports for preamplifiers and connections to wires	90
1.6 Sense- and potential wires	120
1.7 Tools for mounting and stringing	200
1.8 Gas pipes and distribution	40
1.9 Gas mixing apparatus	100
Sum 1	1250
2. Electronics	
2.1 Readout electronics	1980
2.2 Modifications of trigger	100
2.3 HV supply, complete	120
Sum 2	2200
3. Manpower (external)	
3.1 Stringing the wires	300
3.2 Cabling and installation in pit	100
Sum 3	400
Total sum	3850

Table 4. Cost estimates for the SWC

	kDM
1. LAF	
1.1 BGO	600
1.2 Readout electronics and trigger for BGO	300
1.3 BGO container and supports	30
1.4 Tube chambers	25
1.5 Readout electronics for tube chambers	135
Sum 1	1090
2. SAF	
2.1 Modifications of SAF	30
2.2 Supports	30
Sum 2	60
Total sum	1150

Table 5. Cost estimates for the forward detectors

	kDM
1. Modification of the 1983 beampipe	50
2. Beampipe for 1985	
2.1 Inner beryllium part	100
2.2 Beampipe trumpets	50
Sum	200

Table 6. Cost estimates for the beampipe

8.1.2 Cost breakdown

In Tbl. 7 (p.57) we give a total cost breakdown for the costs of the detector components and for the money involved from the members of the collaboration. Their contributions are subject to final approval by funding authorities.

In the period of 1983 to 1985 some additional equipment will be needed which is not included in this proposal. A new He-compressor for the supply of the superconducting coil will be purchased in 1983. Presently a coarse scintillator sandwich is being built which closes the gap between endcap and barrel shower counters ($22° < \vartheta < 30°$). An IBM-370-E-emulator will be installed in the online data acquisition chain. Furthermore a TOF system is being considered.

Component Contributions of	SWC kDM	LAF/SAF kDM	Beam-pipe kDM	Total costs kDM
DESY	1970	30	200	2200
Glasgow	200			200
Hamburg	160	440		600
IN2P3	470	30		500
Karlsruhe	550	250		800
München	500	400		900
Sum	3850	1150	200	5200

Table 7. Total cost breakdown (subject to final approval)

8.2 TIME SCHEDULE

The time schedule is given in Tbl. 8 (p.58) . The characters used in this table have the following meanings: D = design, F = fabrication, T = test, I = installation, W = wire stringing (SWC only). The time schedule assumes an approval of this proposal in spring 1983.

Component	Year/Month		
1. SWC	1983 JJASOND	1984 JFMAMJJASOND	1985 JFMAMJJAS
1.1 Endplates	D-D F-	-FW---------	WT---TII
1.2 Vertex Det.	D---D	F---FW-	WT---TII
1.3 Wiring tools	D-D F--	-F	
1.4 Electronics	D-DF---	----------FT-	T
2. LAF/SAF	JJASOND	JFMAMJJASOND	JFMAMJJAS
2.1 BGO			
crystals	F------	--------F	
tests		T-T T--T	II
2.2 LAF tube ch.	F--	--FT----T	II
2.3 SAF			
active convert.		F----FT-T	I
mod. Pb-Glass			FI
supports		F-F	I
2.4 SAF tube ch.	F---F	T-T	I
3. Beampipe	JJASOND	JFMAMJJASOND	JFMAMJJAS
3.1 '84 beampipe		F	-FI
3.2 '85 beampipe			
inner part	D----DF-	---F	
outer part	D----D		F--F II
	JJASOND 1983	JFMAMJJASOND 1984	JFMAMJJAS 1985

Table 8. Time schedule 1983 - 85

9.0 SUMMARY

In order to meet the requirements of experiments running during the comming years at PETRA, we propose significant modifications to the existing CELLO detector set-up, namely to replace the central track detector and to improve the detectors in the forward region. We are convinced that the parts of the detector, which will not be modified, especially the superconducting coil and the liquid argon calorimeters, are quite appropriate for future experiments.

The proposed central track detector is a cylindrical drift chamber with 36 layers and a total of ~ 7500 wires. All wires have angles of ± 2° with respect to the beam axis. The expected momentum resolution is $\sigma(p)/p^2 \sim 0.005\ GeV^{-1}$, the vertex precision is $\sigma(r_{min}) = 120\ \mu m$. About 23% of the wires are equipped with current division readout to facilitate pattern recognition at small polar angles. Track measurement is possible down to polar angles of $\vartheta \sim 140$ mrad.

To cover the angular region $\vartheta < 130$ mrad at best a two step solution is proposed: a "large angle forward tagger" and a "small angle forward tagger". The large angle forward tagger is an array of BGO crystals with photodiode readout, which has an energy resolution comparable to that of the liquid argon endcap calorimeter. The small angle forward detector is an existing shower counter array. Both detectors have additional tube chambers for improved position measurements.

The proposed hardware is organized such that improvements in the future are possible without major modifications, e.g. there is space for a time of flight counter and we have the option to equip all wires with ADC readout for dE/dx measurement to improve the particle identification.

Beyond the experiments at PETRA we mention here that several items of the CELLO detector have properties which are required for first generation experiments at the HERA collider. The central track detector is designed to disentangle high track densities, the superconducting coil is compact, the liquid argon calorimeters have a fine granularity and are relatively thick. These features are typical of those required for central detectors and electromagnetic calorimeters in experiments to study deep inelastic ep collisions.

A.0 REFERENCES

1. CELLO Collaboration, H.J.Behrend et al., DESY 82-061 (1982);
   JADE Collaboration, W.Bartel et al., DESY 82-086 (1982).

2. CELLO Collaboration, H.J.Behrend et al., Z.Phys. C14, 283 (1982).

3. CELLO Collaboration, H.J.Behrend et al., DESY report, March 1983.

4. TASSO Collaboration, M.Althoff et al., DESY 83-010(1983);
   MarkII-Collaboration, J.M.Yelton et al., SLAC-PUB-2962 (1982).

5. J.H.Field, Proceedings 17th. Rencontre de Moriond, 1982, Vol.1, p.207.

6. J.Haissinski, Proceedings 17th. Rencontre de Moriond, 1982, Vol.2, p.839.

7. TASSO Collaboration, R.Brandelik et al., Z.Phys. C10, 117 (1981);
   J.Olsson, Proceedings 17th. Rencontre de Moriond, 1982, Vol.2, p.13;
   D.L.Burke, Proceedings 21st. Int. Conf. on High Energy Physics, Paris, 1982, PC3-513.

8. C.Edwards et al., SLAC-PUB 2896 (1982)
   K.C.Königsmann, Proceedings 17th. Rencontre de Moriond, 1982, Vol.1, p.63.

9. TASSO Collaboration, R.Brandelik et al., DESY 81-058 (1981).;

10. TASSO Collaboration, M.Althoff et al., DESY 82-071(1982).

11. TASSO Collaboration, R.Brandelik et al., Phys.Lett. 97B, 448 (1980);
    TASSO Collaboration, M.Althoff et al., DESY 82-062(1982).

12. G.Alexander, U.Maor and P.G.Williams, Phys.Rev. D26, 1198 (1982).

13. PLUTO Collaboration, Ch.Berger et al., Phys.Lett. 99B, 287 (1981) and 107B, 168 (1981);
    TASSO Collaboration, R.Brandelik et al., Phys.Lett. 103B, 133 (1981) and 107B, 290 (1981).

14. PLUTO Collaboration, Ch.Berger et al., Phys.Lett. 107B, 168 (1981);
    JADE Collaboration, W.Bartel et al., DESY 82-064 (1982).

15. T.F.Walsh, Phys.Lett. 36B, 121 (1971).

16. JADE Collaboration, W.Bartel et al., Phys.Lett. 107B, 163 (1981);
    TASSO Collaboration, R.Brandelik et al., Phys.Lett. 107B, 290 (1981).

17. W.Allison et al., Ann. Rev. Nucl. Part. Sci., 30, 253 (1980).

18. M.Cavalli-Sforza et al., Proceedings Int. Conf. Colliding Beam Physics, Stanford, Feb. 17-23, 1982 Report SLAC-250 (UC - 34d).

19. E.Lorenz, talk at DESY, Dec. 1,1982.

20. M.Kobayashi et al., KEK preprint 82-9, July 1982.

21. A.Philipp and L.Joensson, ARGUS Collaboration, private comunication.

22. P.Leu, private communication.